THE UNIVERSITY OF MICHIGAN
INDUSTRY PROGRAM OF THE COLLEGE OF ENGINEERING

SHOCK INDUCED CHEMICAL REACTIONS

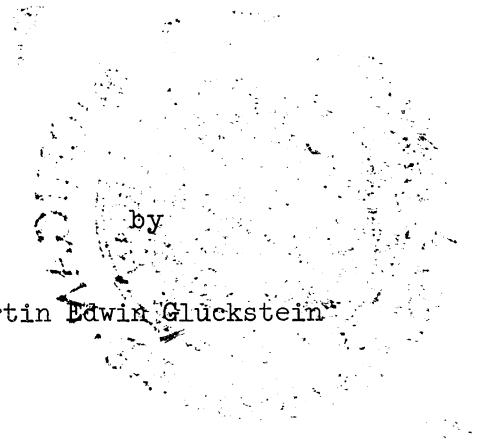

by

Martin Edwin Gluckstein

This dissertation was submitted in partial fulfillment of the requirements for the degree of Doctor of Philosophy in The University of Michigan, 1957.

February, 1957

IP-208

Engn
UMR
1656

Doctoral Committee:

Associate Professor Stuart W. Churchill, Chairman
Associate Professor Richard B. Morrison
Professor Robert R. White
Associate Professor J. Louis York

ACKNOWLEDGEMENT

The author wishes to express his appreciation to the members of the Doctoral Committee for their many helpful suggestions and constant encouragement during the conduct of this work. In addition, Professor C. M. Sliepcevich, presently of the University of Oklahoma, offered significant assistance in the design of the experimental equipment and in the formulation of the problem. Without the contribution of these men, this work never could have been completed.

The research was supported by National Science Foundation Grant G-1112. The author wishes to extend his deep gratitude for this support.

To the shop and laboratory personnel of the Department of Chemical and Metallurgical Engineering, the author expresses his thanks for helpful and faithful assistance in some of the mechanical and analytical problems presented by this problem.

The manuscript was typed and prepared by Mrs. Barbara Ray, whose efficiency and amiable personality materially lessened this chore.

TABLE OF CONTENTS

LIST OF TABLES

LIST OF ILLUSTRATIONS

I. INTRODUCTION

A. Scope of Research

The purpose of this dissertation is to examine the feasibility of promoting chemical reactions by means of shock waves and hydrodynamically related phenomena, to examine the chemical equilibrium of these reactions and to interpret these results in so far as possible in terms of reaction rates and mechanisms. Because of the exploratory nature of the work, attention was directed towards relatively simple reactions whose behavior in ordinary laboratory systems has been fairly well established.

Due to the current, wide interest in the use of shock waves as promoters of chemical reactions and in the use of the shock tube in chemical and chemical engineering research, a fairly extensive review of shock wave literature is presented. A classification system for shock flows with chemical reaction is presented and a technique for the determination of the equilibrium behind such waves is outlined. Detonative processes are considered only insofar as they are related to the general physical structure of shock waves with chemical reaction, and as a method for the generation of strong shock waves.

The problems of the design of experimental equipment for this work are analyzed and the special features of the experimental equipment presented.

B. Review

The existence of shock waves was first suggested on mathematical grounds. According to Courant and Friedrichs (10), Poisson, in 1808 presented a simple wave solution for the flow of an isothermal gas. Challis (6) demonstrated such a solution is not necessarily unique, while Stokes (36) showed that uniqueness is obtained only if it is assumed that a discontinuity occurs in the velocity when the velocity gradient becomes infinite. He further reasoned that such flows could not exist for real gases. (This conclusion is a correct one, in the general sense, and it is only gases which possess no molecular transport properties that a true discontinuity may occur. Indeed, some of the more recent work on the theory of shock waves involves the development of suitable mathematical techniques and physical models to treat the effects of viscosity and related molecular properties.) Earnshaw (13) demonstrated that a compression in a gas satisfying the relation $p = p(\rho)$ would continually gain on itself until a discontinuity is formed. Riemann (32) elaborated this theory on the erroneous assumption that these processes are adiabatic and reversible. Rankine (31) showed that continuous changes from one finite state to another in a steady adiabatic process are not possible and further that heat must be transferred from one particle to another even for a system isolated from its surroundings. This conclusion is consistent with the conservation of energy, but, as pointed out by Rayleigh (33) and Hugoniot (22), is not consistent with the requirements of the second law of thermodynamics. Rayleigh (33) further showed that

the entropy must increase across a shock wave and therefore expansion shocks are not possible.

The actual production of shock waves in a tube may be credited to Vielle (40), although the previous but unidentified occurrence of shock waves in high pressure plumbing or flow devices is certain. The class of combustion phenomena known as detonations were investigated by workers in the late nineteenth century. Chapman (7) and Jouguet (25) independently demonstrated the relation between this class of combustion and the hydrodynamic theory of shock waves.

The literature on this subject is an extensive one and will not be reviewed. Only that information which is germane to this dissertation will be introduced as needed.

The actual application of the shock tube to the study of chemical problems is of such recent interest that The Chemical Abstracts fails to list the indicial headings of "shock tubes" or "shock waves" prior to 1947, and the preponderance of material prior to that date concerns detonations or the initiation of detonations. Since then Kantrowitz and coworkers (35), Laporte and Turner (38), and Zeldovich (42) have reported on the use of shock waves or shock tubes to produce extremely high temperatures. The shock tube technique has also been utilized by Davidson, et al., (4, 5, 18) and by Greene (20) in the study of certain simple decomposition reactions. Hertzberg, Squire, and Glick (19) have reported a special design of a shock tube for the study of high temperature gaseous reactions and have reported data for the system $N_2 + O_2$.

Since the initiation of the present work, the author has learned informally of investigations similar in scope to this one but no other publications in the established literature have come to his attention.*

The information presented in this review is by no means intended to be exhaustive or complete. Compedia such as the Combustion Symposium Volumes (43,44,45) and the books by Lewis and von Elbe (27), Zeldovich (41), and Jost (24) should certainly be mentioned as valuable sources. In addition a bibliography by Elder (14) presents a wealth of source material on the physics of shock waves.

*A Thesis by Bennett (2) issued as a report from the California Institute of Technology has been recently received.

II. THEORY

A. Equation of Motion of Fluid Dynamics

In this section and in the next section, the equations of motion for fluid flow are developed for the case of a time dependent, three dimensional flow, and then specialized to the one dimensional case of the shock tube. The limitations of the equations will be discussed and their application to shock flows with chemical reaction indicated. The development of the equations of fluid flow will follow that of Chapman and Cowling (8) and of Hirschfelder, Curtiss, and Bird (21). They treat the problem by use of the principles of statistical mechanics. This approach, in contrast to the usual treatment developed in the aerodynamic literature, such as Prandtl (30) or Kuethe and Schetzer (26), allows the introduction of the chemical parameters in more realistic fashion.* The penalty for this more fundamental approach is a slightly greater mathematical complexity but none of the shortcomings of the artificial introduction of the chemical parameters are incurred. The resultant equations are the same in both cases but the latter method provides greater physical insight.

The hydrodynamic equations necessary for the solution of any flow problem may be summarized as follows:

(a) An equation of state, usually in the form $P = P(\rho,T)$,

(b) An equation for the conservation of each component specie,

---

*A derivation of these equations for detonations is given by Morrison by extension of the classical aerodynamic equations (28).

(c) An equation for the conservation of mass,

(d) An equation for the conservation of momentum, and

(e) An equation for the conservation of energy.

Consider a system of N molecules of s different components in a fixed Cartesian coordinate system.* Let n_s be the number density of molecules of the s^{th} type and $\underline{V}_s$, the linear velocity of molecules of the s^{th} type with respect to the fixed coordinates. From the kinetic theory of gases

$$\overline{\underline{V}}_s = \frac{1}{n_s} \int_{-\infty}^{\infty} \underline{V}_s \, f_s(\underline{r},\underline{V}_s,t) \, dV_s \tag{1}$$

where $\overline{\underline{V}}_s$ is the average or expectation value of the velocity, dV_s, the volume element in velocity space and $f_s(\underline{r},\underline{V}_s,t)$ a scalar function of $\underline{r}$ and $\underline{V}_s$ called the distribution function.

The mass average or stream velocity, $\underline{V}_o$ is defined as

$$\underline{V}_o(\underline{r},t) = \frac{1}{\rho} \sum_s m_s \, n_s \, \overline{\underline{V}}_s \tag{2}$$

where ρ is the ordinary density of the fluid and m_s, the mass of molecules of the s^{th} kind. Clearly

$$\rho(\underline{r},t) = \sum_s n_s \, m_s = \sum_s \rho_s(\underline{r},t).$$

Defining a quantity $\underline{W}_s(\underline{r},\underline{V}_s,t)$ as the velocity of a molecule relative to an axis moving with the stream velocity or

---

*The coordinates of this space are velocity components and the space is called a velocity space.

$$\underline{W}_s = \underline{V}_s - \underline{V}_o \tag{3}$$

and further the diffusion velocity as the flow rate of molecules of the s^{th} type with respect to $\underline{V}_o$. Clearly this quantity is $\overline{\underline{W}}_s$ and

$$\sum_s n_s\, m_s\, \overline{\underline{W}}_s = \sum_s n_s\, m_s\, (\overline{\underline{V}}_s - \underline{V}_o) = 0 \tag{4}$$

Consider the arbitrary quantity ψ_s which is conserved in molecular encounters and is at the most a function of $\underline{W}_s$. From geometric considerations it may be shown that the flux of ψ_s (i.e., the quantity of ψ per unit area per unit time) is $\psi_s f_s(\underline{n} \cdot \underline{W}_s)dW_s$, where $\underline{n}$ is the unit normal vector. Since $\psi_s = \psi_s(\underline{W}_s)$, the total flux of ψ_s is

$$\underline{\psi}_s \cdot \underline{n} = \int_{\infty}^{\infty} \psi_s\, f_s\, (\underline{n} \cdot \underline{W}_s) dW_s \tag{5}$$

$\underline{\psi}_s$ is therefore the flux vector associated with ψ_s.

If it is assumed the mass, momentum, and energy are independently conserved, then ψ_s may be defined as each of these quantities in turn, and an expression for the flux of mass, momentum, or energy obtained.

(a) Let $\psi_s = m_s$; therefore

$$\underline{\psi}_s = \underline{J}_s = m_s \int_{\infty}^{\infty} f_s\, \underline{W}_s\, dW = n_s\, m_s\, \overline{\underline{W}}_s \tag{6}$$

where $\underline{J}_s$ is the mass flux vector of s and

$$\underline{J} = \sum_s \underline{J}_s$$

(b) Let $\psi_s = E_s$, where E_s is the total molecular energy of the s^{th} specie, then

$$\underline{q}_s = \int_{\infty}^{\infty} E_s\, \underline{W}_s\, f_s\, dW_s \tag{7}$$

where $\underline{q}_s$ is the heat flux vector. The integration of equation (7) requires that E_s be expressed as a function of $\underline{W}_s$. From statistical mechanics, it is possible to express E_s as

$$E_s = \frac{1}{2} m_s W_s^2 + E_s^i$$

where E_s^i is the energy of the internal degrees of freedom of an s molecule. E_s^i is independent of W_s. Expanding E_s as above yields the heat flux vector in the form

$$\underline{q}_s = \frac{1}{2} \int_{-\infty}^{\infty} m_s W_s^2 \underline{W}_s f_s dW_s + \int_{-\infty}^{\infty} E_s^i \underline{W}_s f_s dW_s \tag{8}$$

which reduces to

$$\underline{q}_s = \frac{1}{2} n_s m_s \overline{W_s^2 \underline{W}_s} + \underline{q}_s^i \tag{9}$$

For monotonic gases at sufficiently low temperatures $\underline{q}_s^i = 0$.

(c) If $\psi_s = m_s \underline{W}_{sx}$, the x component of momentum, then

$$\underline{P}_{sx} = m_s \int_{-\infty}^{\infty} \underline{W}_{sx} \underline{W}_s f_s dW_s = n_s m_s \overline{\underline{W}_{sx} \underline{W}_s} \tag{10}$$

where $\underline{P}_{sx}$ is the flux vector associated with the transport of the x component of momentum. Similarly

$$\underline{P}_{sy} = n_s m_s \overline{\underline{W}'_{sy} \underline{W}_s} \tag{11}$$

$$\underline{P}_{sz} = n_s m_x \overline{\underline{W}_{sz} \underline{W}_s} \tag{12}$$

The total momentum flux is a quantity which has as its components the three directional flux vectors and is denoted as $\tilde{P}_s$. Arranging $\tilde{P}_s$ in matrix form

$$P_s = \begin{pmatrix} \underline{P}_{sx} \\ \underline{P}_{sy} \\ \underline{P}_{sz} \end{pmatrix} = m_s n_s \begin{pmatrix} \overline{W_{sx}W_{sx}} & \cdots & \cdots \\ W_{sy}W_{sx} & W_{sy}W_{sy} & \cdots \\ W_{sz}W_{sx} & \cdots & W_{sz}W_{sz} \end{pmatrix} = n_s m_s \overline{\underline{W}_s \underline{W}_s} \qquad (13)$$

The form of equation (13) suggests a relationship between this term and the fundamental equation of the thermodynamics of irreversible processes, which provides for specific relation between the fluxes ($\underline{P}_{si}$), the forces which cause them, and the coupling (interactions) between the components of different fluxes (c.f. De Groot (11)). However, the information provided by these techniques is not sufficiently general, due to the limited applicability of the linear laws required to manipulate the Onsager relations in irreversible thermodynamics. The important results which may be obtained is that in equation (13) $P_{ij} = P_{ji}$, where P_{ij} is the term in the i^{th} row and j column. This same result may be obtained on a simple basis, since P_{ii} are normal stresses on a fluid element and P_{ij} ($j \neq i$) are the shear stresses.

In order to obtain the total fluxes, these results must be summed over all components.

From the kinetic theory of dilute gases, Boltzmann's equation may be written

$$\frac{\partial f_s}{\partial t} + \underline{V}_s \cdot \frac{\partial f_s}{\partial \underline{r}} = \sum_{\sigma} \left(\Gamma^{+}_{s\sigma} - \Gamma^{-}_{s\sigma} \right) \qquad (14)$$

The terms $\Gamma_{s\sigma}^{+}$ and $\Gamma_{s\sigma}^{-}$ are these rates of production and removal of s molecules by collisions of all other type molecules σ; clearly

$$\Gamma_{ss}^{+} - \Gamma_{ss}^{-} \equiv 0$$

and

$$\sum_{\sigma} (\Gamma_{s\sigma}^{+} - \Gamma_{s\sigma}^{-}) = \sum_{\sigma} \Gamma_{s\sigma}^{\pm} = K_s , \tag{15}$$

the volumetric rate of production of s, molecules per unit time per unit volume. Continuity requires that

$$\sum_{s} K_s m_s = 0$$

If the left hand side of (14) is multiplied by ψ_s and integrated over velocity space, then

$$I = \int_{-\infty}^{\infty} \psi_s \left(\frac{\partial f_s}{\partial t} + \underline{V}_s \cdot \frac{\partial f_s}{\partial \underline{r}} \right) dV_s \tag{16}$$

The various terms in (16) may be expanded:

$$\int \psi_s \frac{\partial f_s}{\partial t} dV_s = \frac{\partial}{\partial t} \int \psi_s f_s dV_s - \int f_s \frac{\partial \psi_s}{\partial t} dV_s ; \tag{17}$$

$$\int \psi_s \underline{V}_s \cdot \frac{\partial f_s}{\partial \underline{r}} = \int \psi_s \left\{ V_{sx} \frac{\partial f_s}{\partial x} + V_{sy} \frac{\partial f_s}{\partial y} + V_{sz} \frac{\partial f_s}{\partial z} \right\} dV_s . \tag{18}$$

Equation (18) becomes

$$\int \psi_s V_{sx} \frac{\partial f_s}{\partial x} dV_s = \frac{\partial}{\partial x} \int \psi_s V_{sx} f_s dV_s - \int V_{sx} f_s \frac{\partial \psi_s}{\partial x} dV_s \tag{19}$$

for the x component and similarly for y and z.

By applying the previous definitions of average quantities, one obtains the result

$$\frac{\partial}{\partial t} n_s \bar{\psi}_s + \frac{\partial}{\partial \underline{r}} \cdot n_s \overline{\psi_s \underline{V}_s} - n_s \left(\overline{\frac{\partial \psi_s}{\partial t}} - \overline{\underline{V}_s \cdot \frac{\partial \psi_s}{\partial \underline{r}}} \right) = \sum_\sigma \int \psi_s \Gamma^{\pm}_{\sigma s} \, dV_s \qquad (20)$$

As before we let ψ_s take the values m_s, $m_s \underline{W}_s$ and E_s.

(a) If $\psi_s = m_s$, then

$$\frac{\partial n_s}{\partial t} + \frac{\partial}{\partial \underline{r}} \cdot n_s \bar{\underline{V}}_s = K_s = \frac{\partial n_s}{\partial t} + \frac{\partial}{\partial \underline{V}} \cdot n_s (V_o + \bar{\underline{W}}_s) \qquad (21)$$

and by summing over s

$$\frac{\partial \rho}{\partial t} + \frac{\partial}{\partial \underline{r}} \cdot \rho V_o = 0 \qquad (22)$$

Equation (22) is the well known continuity equation.

(b) If $\psi_s = m_s \underline{W}_s$ and we again sum over all s, then

$$\sum_s m_s \left\{ \frac{\partial}{\partial t} n_s \bar{\underline{W}}_s + \frac{\partial}{\partial \underline{r}} \cdot n_s \overline{\underline{V}_s \underline{W}_s} - n_s \overline{\frac{\partial \underline{W}_s}{\partial t}} - n_s V_s \cdot \frac{\partial}{\partial \underline{r}} \underline{W}_s \right\} = 0 \qquad (23)$$

since

$$\sum_s \sum_\sigma \int \Gamma^{\pm}_{s\sigma} m_s \underline{W}_s \, dV_s = 0$$

Using the definition of $\underline{W}_s$ in terms of $\underline{V}_o$ and $\underline{V}_s$ and the relation

$$\frac{\partial}{\partial \underline{r}} \cdot \rho \underline{AB} = \frac{\partial}{\partial \underline{r}} \cdot \rho \underline{A} + \rho \underline{A} \cdot \frac{\partial}{\partial \underline{r}} \underline{B} \ ,$$

the result

$$\frac{\partial}{\partial t} \rho \underline{V}_o + \frac{\partial}{\partial \underline{r}} \cdot \rho \underline{V}_o \underline{V}_o + \frac{\partial}{\partial \underline{r}} \cdot \tilde{P} = 0 \qquad (24)$$

is obtained by expansion.

Introducing the previously derived continuity equation yields

$$\frac{\partial}{\partial t}\underline{V}_o + \underline{V}_o \cdot \frac{\partial}{\partial \underline{r}}\underline{V}_o = -\frac{1}{\rho}\frac{\partial}{\partial \underline{r}} \cdot \tilde{P} \tag{25}$$

(c) If $\psi_s = E_s$, one has similarly

$$\rho \frac{\partial E}{\partial t} + \rho V_o \cdot \frac{\partial}{\partial r} E = -\frac{\partial}{\partial \underline{r}} \cdot \underline{q} - \tilde{P} : \frac{\partial}{\partial \underline{r}}\underline{V}_o \tag{26}$$

where : indicates the operation $\left(\tilde{P} \cdot \frac{\partial}{\partial \underline{r}}\right) \cdot \underline{V}_o$.

These equations are quite general and are subject only to the limitations inherent in kinetic theory and the assumption of a continuous medium. Although they have been derived only for the case of a dilute gas, they apply equally well for the case of the dense gas. The essential difference in the derivation for the two cases is that a more complicated (and exact) form of the Boltzmann equation is required to describe the dense gas. The form of the terms leading to the irreversibilities in the flows (the fluxes $\underline{J}$, $\underline{q}$, $\tilde{P}$ and the species rate of production, K_s), remain to be determined. If one would assume the application of the linear laws of irreversible thermodynamics, it would be possible to show that the fluxes are proportional to the gradients of concentration, velocity and temperature and thereby obtain the Navier-Stokes form of the equations of motion. No such approximation can be made for the case of K_s, except very near equilibrium, since the rate of production of a material due to chemical reaction is known to depend in a non-linear fashion on the concentrations and temperature. Furthermore,

the linear laws are at the best an approximation, and there is some doubt as to the applicability of the Navier-Stokes equations under shock conditions in real gases.

The energy equation, (26), may be simplified by recalling that $E = \frac{1}{\rho} \sum_s n_s m_s E_s$ and that E_s may be approximated as

$$E_s = C_{vs} T \tag{27}$$

where C_{vs} is the heat capacity at constant volume of the s^{th} specie and T is the temperature in degrees absolute. Substituting in equation (26) and making use of the specie continuity equation, (21), yields

$$\rho C_v \left[\frac{\partial T}{\partial t} + V_o \cdot \frac{\partial T}{\partial \underline{r}}\right] = - \frac{\partial}{\partial \underline{r}} \cdot \underline{q} - \tilde{\underline{P}} : \frac{\partial}{\partial \underline{r}} V_o - \sum_s m_s E_s K_s + \sum_s E_s \frac{\partial}{\partial \underline{r}} \cdot n_s m_s \overline{\underline{W}}_s \tag{28}$$

Equation (28), together with the continuity equation, (22), the specie continuity equation (21) and the momentum equation (25), serve to define a set of equations relating the dynamic variables of the system, providing some statement can be made as to the form of the fluxes. However, one additional equation is needed, namely an equation of state. Functionally, this equation is of the form $P = P(\rho, T)$. Although any form of this equation should permit a solution of the complete equations of motion, analytic solutions become possible only for the trivial case ρ = constant and for the case of the ideal gas

$$P_T = RT \tag{29}$$

or, from the definition of the mass density

$$P = \rho RT \tag{30}$$

where τ is the specific volume, R_o the universal gas constant, ρ the mass density, and R the universal gas constant divided by the molecular weight of the gas.

If one specializes these equations to the case of a one dimensional flow, then

$$\frac{\partial n_s}{\partial t} + \frac{\partial}{\partial x} n_s V_s = K_s \qquad \text{(specie continuity)} \qquad (31)$$

$$\frac{\partial \rho}{\partial t} + \frac{\partial}{\partial x} \rho V_o = 0 \qquad \text{(continuity)} \qquad (32)$$

$$\frac{\partial V_o}{\partial t} + V_o \frac{\partial V_o}{\partial x} = -\frac{1}{\rho} \frac{\partial}{\partial x} \tilde{P} \qquad \text{(momentum)} \qquad (33)$$

and

$$\rho C_v \frac{\partial T}{\partial t} + V_o \frac{\partial T}{\partial x} = -\frac{\partial q}{\partial x} - P \frac{\partial}{\partial x} V_o - E_s m_s K_s + E_s \frac{\partial}{\partial x} n_s m_s \bar{W}_s$$

$$\text{(energy)} \qquad (34)$$

The equation of state is, of course, unaffected by the dimensionality of the flow.

Consider now a steady non-dissipative (isentropic) process in which pressure waves are generated in a tube (standing sound waves). From (32) and (33)

$$V^2 d\rho = dP \qquad (35)$$

or

$$v = a = \left(\frac{\partial P}{\partial \rho}\right)_s^{\frac{1}{2}} \qquad (36)$$

The quantity a is called the speed of sound and is the velocity of propagation of an infinitesimal wave in a medium. That actual sound waves in

ordinary gases are isentropic is shown, from physical reasons, by Zemansky (47). For ideal gases

$$a = \sqrt{\gamma RT} \tag{37}$$

Consider now a large amplitude pressure wave in a tube, as shown in Fig. 1a. Since all points on the wave must travel at their local sonic velocities, the speed of sound at the crest will increase above that at the troughs and the top of the wave will overtake the bottom, as shown in Fig. 1b. Eventually, the slope of the head end will approach infinity and at that point a shock wave is said to have formed (Fig. 1c).

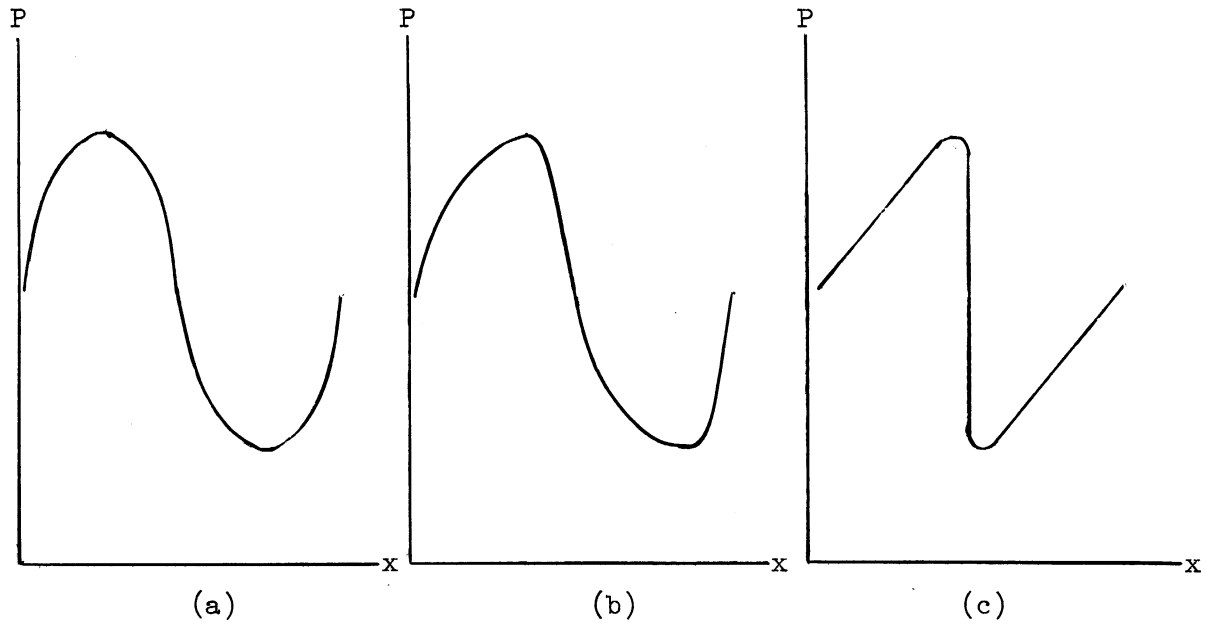

Fig. 1. Formation of shock waves from large amplitude waves.

Physically, there are other ways of generating shock waves, other than by large amplitude disturbances. One such way is by use of a simple device called the shock tube, which will be discussed at length.

B. Shock Waves in Perfect Gases

If we now consider a flowing gas in which the pressure tensor has the form $\tilde{P} = P$, the hydrostatic pressure, and for which $\underline{q} = 0$, and if we further assume the gas to be nonreactive and ideal, we may derive several useful relationships about shock waves in such a system. The flow will be considered one dimensional and flowing from left to right; V is the (local) free stream velocity, P the pressure, ρ the density, and T the absolute temperature. For the steady state, equation (32) becomes

$$\frac{d\rho V}{dx} = 0 \tag{38}$$

which integrates directly to

$$\rho V = \text{constant}_1 = A \tag{39}$$

Similarly, the momentum equation becomes

$$\rho V \frac{dV}{dx} + \frac{dP}{dx} = 0 \tag{40}$$

which has the integral

$$AV + P = \text{constant}_2 = B \tag{41a}$$

or

$$\rho V^2 + P = B \tag{41b}$$

The energy equation (34) for one dimensional, steady flow is

$$\rho V \frac{dE}{dx} + P \frac{dV}{dx} = 0 \tag{42}$$

which further reduces to

$$\rho V \frac{dE}{dx} + \frac{d(PV)}{dx} + \rho V^2 \frac{dV}{dx} = 0 \tag{43}$$

if one uses the definition of the derivative of a product and equation (40). By integration (43) becomes

$$A\left(E + \frac{P}{\rho} + \frac{V^2}{2}\right) = \text{constant}_3 = C \tag{44}$$

or

$$H + \frac{V^2}{2} = H_o \tag{45}$$

where H is the specific enthalpy. If the system is composed of reacting components, equations (39), and (41a) remain unchanged. Equation (45) is still correct but a more useful form may be developed.

For perfect gases of the s^{th} type

$$H_s = C_{ps}T + H_s^o \tag{46}$$

where H_s^o is the enthalpy of formation of s at 0°K. For a mixture of perfect gases

$$H = \frac{1}{\rho}\sum_s m_s n_s H_s \tag{47}$$

and by substitution of (47) and (46) into (45) yields the result

$$\left(\sum_s m_s n_s C_{ps} T + \sum_s m_s n_s H_s^o + \frac{\rho V^2}{2}\right)_1 = \left(\sum_s m_s n_s C_{ps} T + \sum_s m_s n_s H_s^o + \frac{\rho V^2}{2}\right)_2 \tag{48}$$

But

$$\rho^{-1}\sum_s m_s n_s C_{ps} = C_p$$

and one may define a function

$$Q = \rho^{-1}\sum_s m_s n_s (H_{s1}^o - H_{s2}^o) \tag{49}$$

the negative of the enthalpy of formation at 0°K multiplied by an appropriate "extent of reaction". Clearly then

$$Q + C_{p_1} T_1 + \frac{V_1^2}{2} = C_{p_2} T_2 + \frac{V_2^2}{2} \tag{50}$$

a form of the energy equation which is useful for reacting systems. In deriving equation (50) no provision was made for a finite reaction rate

and indeed this equation is only valid for states 1 and 2 being states of thermodynamic equilibrium. For a finite reaction rate, equation (50) is no longer valid and the more general forms of the equations derived in the previous section are needed.

Because of the techniques employed in the derivation of these equations [(39), (41), and (45) or (50)] they are often called the first integrals of the equations of motion. It would appear that they can no longer be integrated, but it will be shown that more general forms of the heat flux vector and the pressure tensor introduce higher order derivatives in the one dimensional equations. These equations are also called the "jump equations" and have been used to develop relations between the states of the gases on both sides of shock or reaction waves, particularly detonations. For convenience they are grouped below:

$$\rho_1 V_1 = A = \rho_2 V_2 \tag{39}$$

$$P_1 + \rho_1 V^2 = B = P_2 + \rho_2 V^2 \tag{41b}$$

$$H_1 + \frac{V_1^2}{2} = H_o = H_2 + \frac{V_2^2}{2} \tag{45}$$

or

$$H_1 + \frac{V_1^2}{2} + Q = H_2 + \frac{V_2^2}{2} \tag{50}$$

where $H = C_p T$.

From equations (39), (41), and (45), one may show that*

$$\frac{P_2}{P_1} = \frac{2\gamma}{\gamma+1} M_s^2 - \frac{\gamma-1}{\gamma+1} \tag{51}$$

---

*Since the derivation of these equations is well known and has been presented in various other works, it will be reserved for the Appendix of this dissertation.

$$\frac{\rho_2}{\rho_1} = \frac{V_1}{V_2} = \frac{1 + \frac{\gamma+1}{\gamma-1}\frac{P_2}{P_2}}{\frac{\gamma+1}{\gamma-1} + \frac{P_2}{P_1}} \tag{52}$$

$$M_2^2 = \frac{1 + \frac{\gamma-1}{2} M_1^2}{\gamma M_1^2 - \frac{\gamma-1}{2}} \tag{53}$$

and

$$\frac{P_2\rho_1}{P_1\rho_2} = \frac{T_2}{T_1} \tag{54}$$

where $M = V/a$, the Mach number, and the subscripts 1 and 2 refer to conditions ahead of and behind the wave, respectively.

The basic properties of pure shock wave may be examined with reference to equations (51) - (54). From the definition of the entropy of an ideal, perfect gas one may show that

$$S_2 - S_1 = \frac{1}{\gamma(\gamma-1)} \ell n \left(\frac{2\gamma}{\gamma+1} M^2 - \frac{\gamma-1}{\gamma+1} \right) \left(\frac{1 + \frac{\gamma-1}{2} M^2}{\frac{\gamma+1}{2} M^2} \right)^{\gamma} \tag{55}$$

The shock strength P_2/P_1 is given by equation (51) and from it one may determine the density and temperature ratios. In Table I, the temperatures behind shock waves of various intensities (T_{2s}) are compared to the temperatures which would be attained by isentropic compression to the same pressure ratio (T_{2isen}). The initial conditions are T = 273 °K and the gas is air, $\gamma = 1.4$. The effects of dissociation are neglected.

TABLE I*

PROPERTIES OF SHOCK WAVES IN AIR

Shock Strength	Density Ratio	T_{2s}	T_{2isen}	Mach Number of Shock
2	1.63	336	330	1.3
5	2.84	482	426	2.05
10	3.88	705	515	2.81
50	6.04	2260	794	6.17
100	7.66	3860	950	8.70
1000	14.30	19100	1710	26.50

It is clearly seen from Table I that it is possible to attain rather high temperatures in gases without the need for heat exchange equipment, if it is possible to propagate strong shock waves through the gas.

C. The Shock Tube

A device commonly used on the laboratory for the generation of single shock waves is called the shock tube. Fig. 2 is a schematic diagram of a shock tube, and it consists of a high pressure and low gas reservoir separated by a diaphragm.

*From Döring (12).

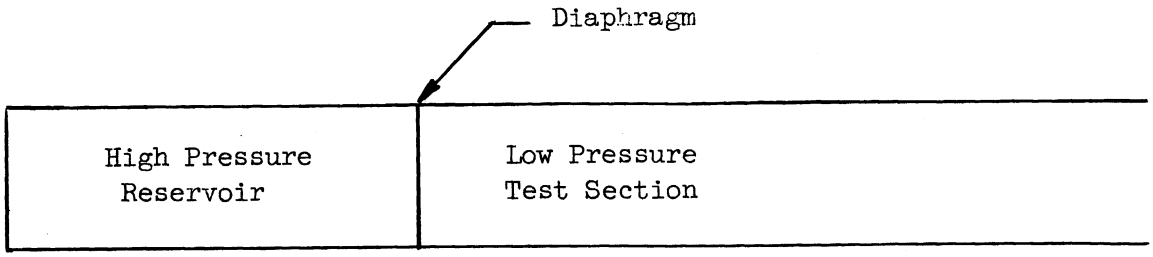

Fig. 2. Schematic diagram of basic shock tube components.

When the diaphragm separating the high and low pressure sections is removed by bursting, a shock wave will propagate into the stagnant, low pressure section. The strength of the shock wave will be determined by the pressure ratio across the diaphragm and the states of the gas on each side. The operational characteristics are clearly transient and a description of the flow must be made with reference to both time and space.

In order to develop equations to determine the flow in a shock tube, the energy equation (34) is transformed to

$$\frac{\partial S}{\partial t} + V \frac{\partial S}{\partial s} = 0 \qquad (56)$$

where S is the specific entropy (See Ref. 21). This equation implies that the entropy of each particle remains constant but each particle may differ in entropy from its neighbor. This form of the energy equation is particularly convenient for mathematical manipulation.

The form of the equations of motion for the one dimensional, unsteady case can be shown to be hyperbolic. For equations of this type there exists a set of curves, called characteristics, in the x-t plane along which solutions of the equations are propagated. Since the theory of characteristics is available elsewhere, only the results will be used in the body of this dissertation. The salient features of the derivation of the characteristic equations will be given in the Appendix.*

By suitable manipulation of the equations of change, it can be shown that the equations of the characteristic lines are

$$\frac{dx}{dt} = (u \pm a) \tag{57}$$

where u and a are the local stream and sonic velocities and dx/dt is the velocity of propagation of a wave. Equation (57) implies that the velocity of a wave in the x-t plane is represented as motion along the lines $(u \pm a)$. The quantities $(u \pm a)$ or quantities linearly related to it are called Riemann invarients, since along any characteristic they are constant. If we call C_+ and C_- the characteristics associated with the positive and negative sign of the Reimann invarient, then the x-t plane may be visualized as being covered with a network of characteristics. Such a diagram is quite convenient for the solution of one dimensional, unsteady flows and is called a wave diagram.

---

*Derivations of the characteristic equations for shock tube flows have been given by Hirschfelder (21), and Courant and Friedrichs (10).

Let us now consider a solution for the flow in a shock tube, such as is shown in Fig. 2. Let region 1 be the undisturbed, low pressure gas; 2, the undisturbed reservoir gas; 3, the region of hot flow behind the shock but ahead of the interface; and 4, the gas between the interface and the rarefaction foot (see Figs. 3a, b, c). At time t = 0, a P-x plot will appear as shown in Fig. 3a. At some time t after the diaphragm has burst, the P-x plot will appear as in Fig. 3b. Fig. 3c represents the wave diagram for the initial wave phenomena in the shock tube and it is from the wave diagram that the P-x plots may be derived.

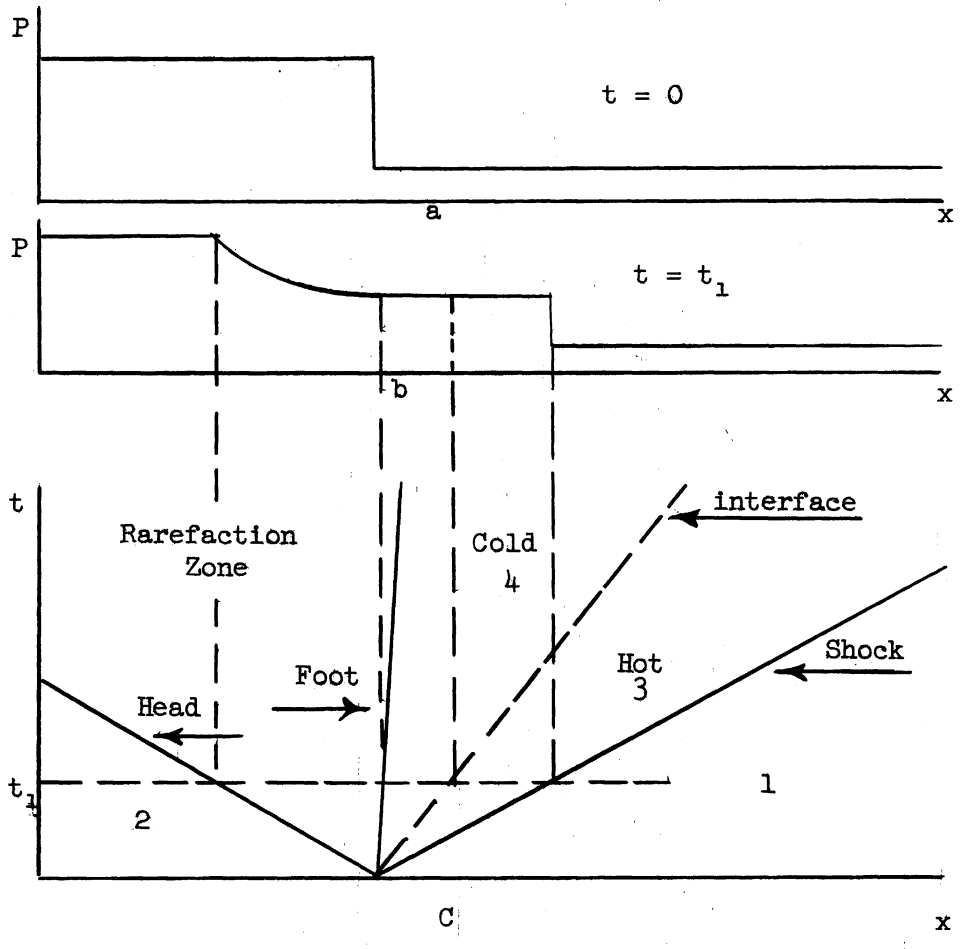

Fig. 3 Wave diagram and P-x plots for a shock tube.

Following Courant and Friedrichs (10) we have

$$u_3 = u_1 \pm \frac{(\beta-1)\left(\frac{P_3}{P_1} - 1\right) a_1}{\left[(\beta+1)\left(1+\beta\frac{P_3}{P_1}\right)\right]^{\frac{1}{2}}} \tag{58}$$

or

$$u_3 = u_1 \pm \mathcal{J}\left(\frac{P_3}{P_1}\right) \tag{58a}$$

where

$$\beta = \frac{\gamma + 1}{\gamma - 1} .$$

Equations (58) or (58a) expresses the velocity behind the shock wave in terms of the shock strength and the initial state of the gas.

Similarly, for the rarefaction

$$u_2 = u_4 \pm \mathcal{R}(P_4/P_2) \tag{59a}$$

or

$$u_2 = u_4 \pm (\beta-1)\, a_2\left[\left(\frac{P_4}{P_2}\right)^{\frac{1}{\beta+1}} - 1\right] \tag{59b}$$

At any point along the expansion zone, the state variables are connected by isentropy. This solution is valid only for a centered rarefaction, that is, one for which all the characteristics meet at a point (Fig. 3c).

Across the interface separating regions 3 and 4, we have

$$u_3 = u_4 \qquad \text{and} \qquad P_3 = P_4 .$$

Or since $u_1 = u_2 = 0$

$$\mathcal{J}\left(\frac{P_3}{P_1}\right) = -\mathcal{R}\left(\frac{P_3}{P_2}\right) \tag{60}$$

Therefore

$$\frac{(\beta_1-1)\left(\frac{P_3}{P_1}\right)a_1}{\sqrt{(\beta_1+1)\left(1+\beta_1\frac{P_3}{P_1}\right)}} = (\beta_2-1)\,a_2\left[1-\left(\frac{P_3}{P_2}\right)^{\frac{1}{\beta_2+1}}\right] \tag{61}$$

and one may solve for the diaphragm pressure ratio in terms of the shock strength. This solution is

$$\pi_{21} = \pi_{31}\left[1-\frac{a_1}{a_2}\cdot\frac{(\beta_1-1)}{(\beta_2-1)}\cdot\frac{(\pi_{31}-1)}{\sqrt{(\beta_1+1)(1+\beta_1\pi_{31})}}\right]^{-(\beta_2+1)} \tag{62}$$

where $\pi_{ij} = P_i/P_j$ and $\pi_{ij} = \pi_{ji}^{-1}$. In terms of the shock Mach number, equation (62) becomes

$$\pi_{21} = \pi_{31}\left\{1-\frac{(\gamma_2-1)\,a_1\,(\pi_{31}-1)\,M_s}{(\gamma_1-1)\,a_2\,(1-\beta_1\pi_{31})}\right\}^{-\frac{2\gamma_2}{\gamma_2-1}} \tag{63}$$

Equations (62) and (63) may be termed "capability equations", since they express the shock strength in terms of the diaphragm pressure ratio.

From equation (62), one may compute the maximum shock strength in a shock tube.* Clearly this value is attained if $\pi_{21}\rightarrow\infty$ or

$$1-\frac{a_1(\beta_1-1)(\pi_{31}-1)}{a_2(\beta_2-1)\sqrt{(\beta_1+1)(1+\beta_1\pi_{31})}}\rightarrow 0 \tag{64}$$

---

*This equation is valid only if the conditions in region 1 are $T\neq 0$, $P\neq 0$.

The possibility that $\pi_{31} \to \infty$ as $\pi_{21} \to \infty$ is ruled out by the limit process. Setting (64) equal to zero as a limit, we have

$$\frac{a_1(\beta_1-1)(\pi_{31}-1)}{a_2(\beta_2-1)\left[(\beta_1+1)(1+\beta_1\pi_{31})\right]^{\frac{1}{2}}} = 1 \qquad (65)$$

From the definition of the speed of sound, we may introduce the temperature and the molecular weight and obtain

$$\left(\frac{\mathcal{M}_2}{\mathcal{M}_1}\right)^{\frac{1}{2}} \frac{(\beta_1+1)(\beta_1-1)}{(\beta_2+1)(\beta_2-1)} \left(\frac{T_1}{T_2}\right)^{\frac{1}{2}} \cdot \frac{\pi_{31\max}-1}{\left[(\beta_1+1)(1+\beta_1\pi_{31\max})\right]^{\frac{1}{2}}} = 1 \qquad (66)$$

Examination of equation (66) shows that the maximum shock strength in the test section would occur if hydrogen is used as a driver gas. The maximum shock strength is also extremely sensitive to the ratio β_1/β_2. In Fig. 4 the maximum shock strength is plotted for $\beta_1=\beta_2=6$ and $\beta_1=6$, $\beta_2=4$ at parameters of T_1/T_2 as a function of $\mathcal{M}_1/\mathcal{M}_2$. The effect of these parameters in determining $\pi_{31\max}$ is clearly seen. Since it is of course impossible to operate at $\pi_{21} = \infty$, the behavior of actual shock tubes (assuming ideal, perfect gases!) would be determined from equation (63). The effect of the parameters $\mathcal{M}_1/\mathcal{M}_2$, T_1/T_2, β_1 and β_2 is seen in Figs. 5 and 6. The Mach number of the shock wave of any strength is calculated from equation (51).

Re-examination of Fig. 3c shows that unless both the test section of a shock tube and the reservoir are infinitely long, the P-x plot shown in Fig. 3b cannot be maintained. Depending upon the type of terminations on the tube, there will be various reflected and transmit-

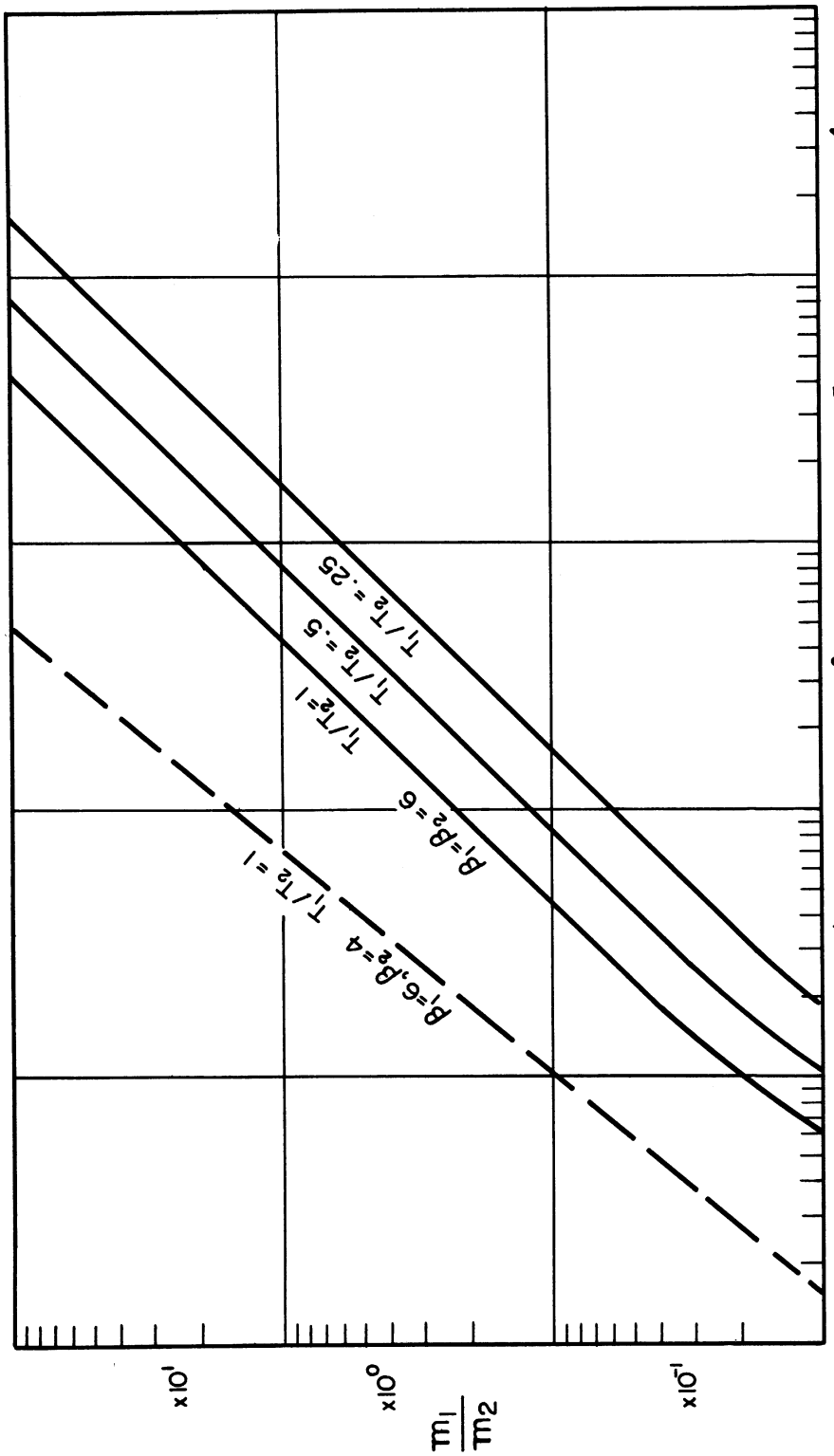

Fig. 4. Maximum shock strength in a shock tube as a function of m_1/m_2 at parameters of β_1, β_2, and T_1/T_2.

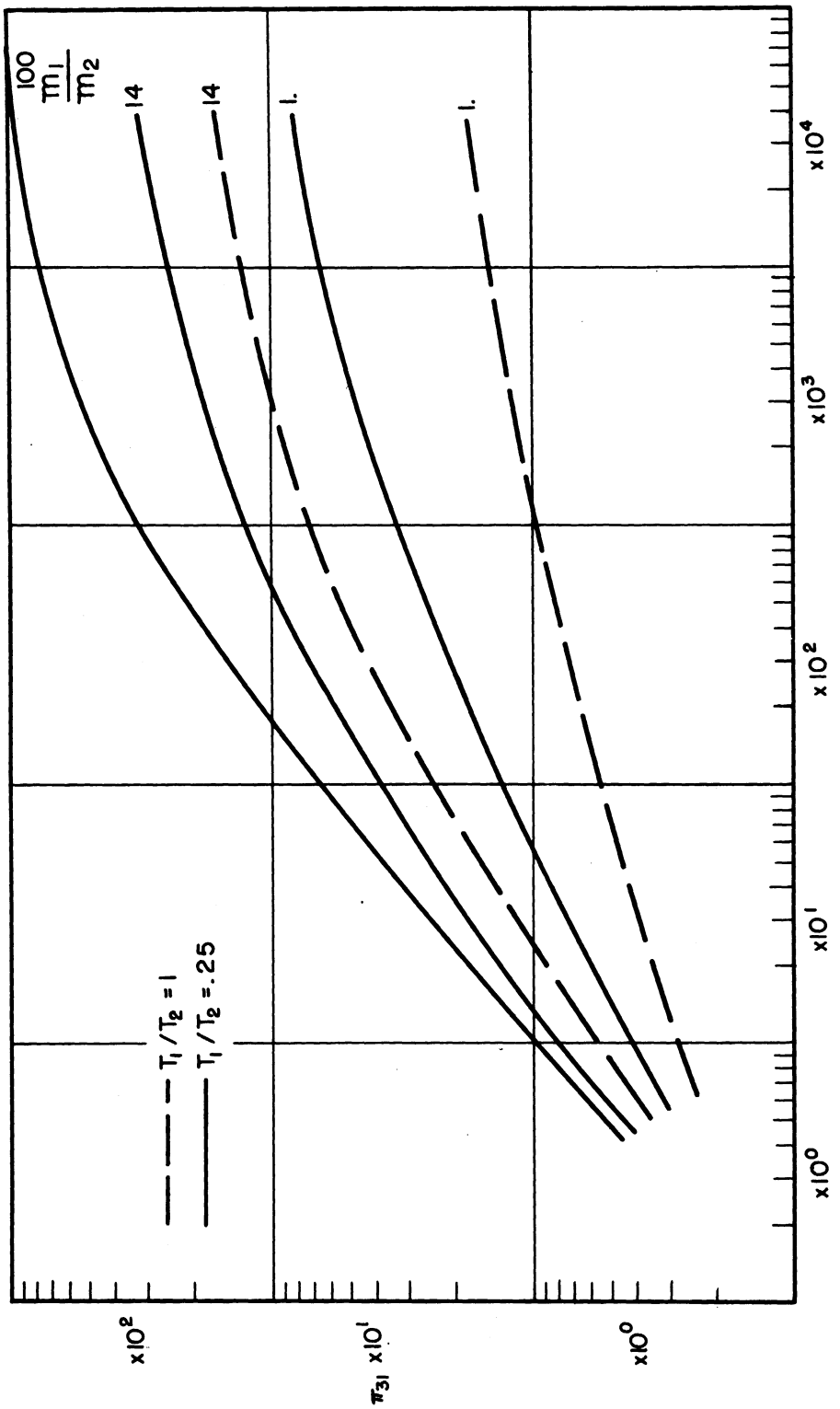

Fig. 5. Shock strength as a function of diaphragm pressure ratio for $\beta_1 = \beta_2 = 6$ with parameters of T_1/T_2 and m_1/m_2.

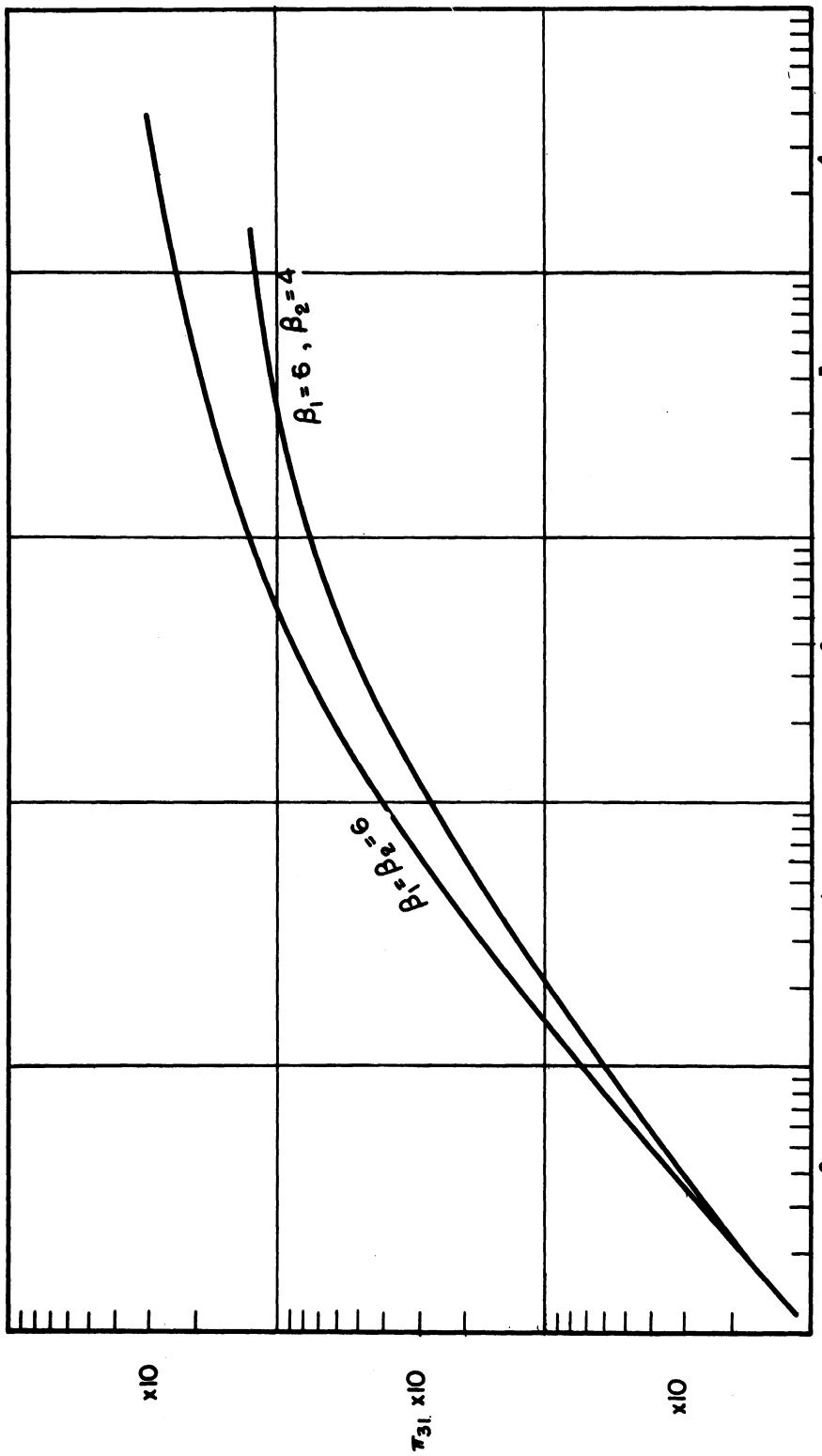

Fig. 6. Shock strength as a function of diaphragm pressure ratio for $\beta_1=\beta_2=6$ and $\beta_1=6$, $\beta_2=4$.

ted waves formed as the primary shock approaches its end of the tube and the rarefaction approaches its end. The general analysis of interaction phenomena is beyond the scope of this thesis and only the specific interactions and terminations which might occur in the equipment used in the experimental portion of this work will be considered. Such consideration will be deferred.

D. Reaction Waves in Perfect Gases

In the preceeding section we have considered the pure shock waves in nonreacting gases in which thermodynamic equilibrium exists on both sides of the wave. This approach is of course an extreme oversimplification, since for strong shock waves it would be expected that the temperature rise would tend to cause dissociation equilibrium on the high pressure side of the wave. Clearly for this case $Q \neq 0$ and derivations based on the simple form of the energy equation will be in error.

Let us now consider the case where $Q \neq 0$ and where the chemical specie on the high pressure side of the wave differ from those on the low pressure side. For convenience, shock waves in which reaction occurs will be called reaction waves and the modifier exothermic applied to those where $Q > 0$ and endothermic to those where $Q < 0$.*

---

*The additional modifiers subsonic or supersonic should also be applied; but since this work is concerned only with the supersonic variety, there is no ambiguity introduced by dropping "supersonic".

The basic equations for the description of these waves are

$$\rho_1 V_1 = \rho_2 V_2 \tag{39}$$

$$\rho_1 + \rho_1 V_1^2 = \rho_2 + \rho_2 V_2^2 \tag{41b}$$

$$H_1 + \frac{V_1^2}{2} + Q = H_2 + \frac{V_2^2}{2} \tag{50}$$

where Q is defined by equation (49). The equation of state may still be written as

$$P = \rho RT \tag{30}$$

with R being evaluated for the average molecular weight of the gases on each side of the wave.

These equations are not in themselves sufficient to solve for the state behind a reaction wave. It is necessary to introduce the equilibrium constant for the reacting system as a function of the temperature, and then to solve the system of simultaneous equations for the state behind the wave.

By combination of (39) and (41b)

$$\frac{P_2 - P_1}{\tau_2 - \tau_1} + C = 0; \quad C = -(\rho_1 V_1)^2 = -(\rho_2 V_2)^2 \tag{67}$$

where τ_1 and τ_2 are the specific volumes. Thus from considerations of mass and momentum conservation along one may conclude that in all waves the change of pressure and specific volume must be of a different sign. It can be shown that $P_2 > P_1$ corresponds to supersonic waves. Equation (50) gives the result called the Hugoniot equation,

$$H_1 - H_2 + Q = \frac{1}{2}(P_1 - P_2)(\tau_2 + \tau_1) \tag{68}$$

and from thermodynamic considerations

$$H = H(P,\tau)$$

therefore equation (68) is an equation which gives the state behind the wave as a function of the state ahead of the wave and a parameter Q. Assume again polytropic gases and a constant Q. The enthalpy is

$$H = \frac{\beta + 1}{2} P\tau$$

and from (68)

$$\beta_1 P_1 \tau_1 + 2Q = \beta_2 P_2 \tau_2 + P_1 \tau_1 - P_2 \tau_2 \qquad (69)$$

If equation (69) is plotted in the P-τ plane, one obtains a family of hyperbolas with Q as a parameter, and (P_1, τ_1) as the initial point, as shown in Fig. 7. The regions II and IV are areas in which equation (69) has no meaningful solution, since in these regions P 0 when ρ 0. It is noted that energy considerations along do not exclude solution in II and IV but that the mass and momentum requirements do.

Regions I and III, in which solutions are permitted, are each further separated into subregions by the line Q = 0, i.e., pure shocks or pure expansions. These subregions, A and B correspond to the exothermic and endothermic cases, respectively.

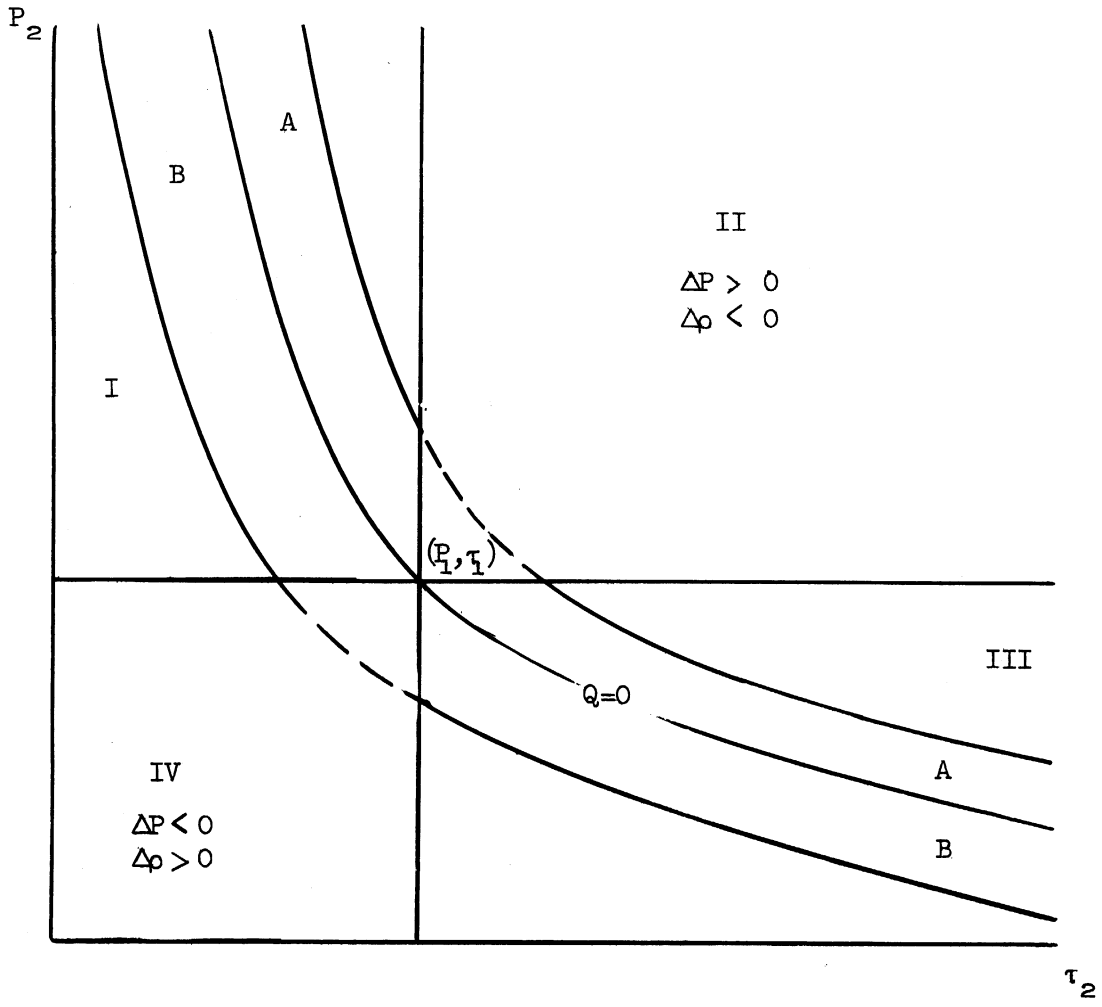

Fig. 7. Hugoniot plot for wave processes.

For any initial point, one has limiting values of Q, determined from the equation

$$\tau_2 = \frac{\beta_1 \tau_1 (P_1+P_2) + 2Q}{\beta_2 P_2 + P_1} \tag{70}$$

as follows. In (70) the numerator and denominator must be positive which implies

$$\beta_1 \tau_1 (P_1+P_2) + 2Q \geq 0$$

or

$$-\frac{\beta_1 \tau_1 (P_1+P_2)}{2} = Q_{min}$$

which rearranges to

$$-\frac{\beta_1 R_1 T_1 (1-\pi_{s1})}{2} = Q_{min}$$

where π_{s1} is the shock strength. Thus it may be concluded that the extent of an endothermic reaction is limited by the strength of the wave.

For both the endothermic and the exothermic waves, the determination of the states behind the wave requires an iterative solution of the hydrodynamic equations and the equations of thermodynamic equilibrium. Some useful solutions for reactions waves will now be derived.

Solving the Hugoniot equation (equation (69)) for the density ratio yields

$$\frac{\rho_b}{\rho_a} = \frac{\pi_{ba}\beta_b - 1}{\pi_{ba} + \beta_a + \Delta} \tag{71}$$

where Δ is defined as $2Q/R_a T_a$. From Appendix A, equation (A.29)

$$\left(\frac{\pi_{ba}-1}{1-\rho_a/\rho_b}\right) P_a \rho_a = \left(\frac{\rho_b-\rho_a}{u_b-u_a}\right)^2$$

or

$$(u_b-u_a)^2 = \frac{P_a}{\rho_a} \frac{(\rho_b/\rho_a - 1)}{\rho_a/\rho_b} (\pi_{ba}-1) \tag{72}$$

where u_a and u_b are the absolute velocities on the low and high pressure sides of the wave, respectively. But, from the equation of state

$$\frac{P}{\rho} = RT$$

and therefore

$$(u_b-u_a)^2 = R_a T_a \left\{\frac{\pi_{ba}(\beta_b-1)+1-\beta_a-\Delta}{\pi_{ba}\beta_b+1}\right\} \{\pi_{ba}-1\} \tag{73}$$

Similarly, the wave velocity is found to be

$$(U-u_a)^2 = R_a T_a \left\{ \frac{\pi_{ba}\beta_b+1}{\pi_{ba}(\beta_b-1)+1-\beta_a-\Delta} \right\} \left\{ \pi_{ba}-1 \right\} \tag{74}$$

Defining the relative Mach number as

$$\frac{U - u_a}{a_a} = M_a$$

then

$$\gamma_a M_a^2 = \left(\frac{\pi_{ba}\beta_b+1}{\pi_{ba}(\beta_b-1)+1-\beta_a-\Delta} \right) \left(\pi_{ba}-1 \right) \tag{75}$$

These equations show the effect of the reacting mixture on the shock properties for a given strength wave. For an endothermic wave, with $\beta_b \geq \beta_a$, and for a given shock strength the density ratio and velocity jump are increased and the wave velocity decreased from those of a pure shock wave. For the exothermic wave, with $\beta_b \leq \beta_a$, the results are opposite. No general conclusion can be drawn when the inequalities in β are in the opposite manner.

In the shock tube, the wave velocity is the quantity most usually and readily measured, and it would be useful to invert equation (74) or (75) to express the pressure ratio as a function of the Mach number. This inversion yields the following equation for π_{ba}.

$$\pi_{ba} = \frac{(\beta_b-1)(1+\gamma_a M_a^2) \pm \sqrt{(1-\beta_b)^2(1+\gamma_a M_a^2)^2+4\beta_b\left[\gamma_a M_a^2(1-\beta_a-\Delta)+1\right]}}{2\beta_b} \tag{76}$$

This equation contains the two unknown parameters Δ and β_b, both of which must be determined. From the equation of state

$$T_b = \pi_{ba} \frac{\rho_a}{\rho_b} T_a \frac{\mathcal{M}_b}{\mathcal{M}_a} \tag{77}$$

and thus it appears that the unknown quantities are

$$\rho_b, P_b, \mathcal{M}_b, T_b, \beta_b, \text{ and } \Delta$$

or there are six unknowns and only three equations. However, of these unknown quantities, the last four are related by the requirements of chemical equilibrium and by specie continuity. The parameter Q or its linear relative Δ are the single terms which relate the chemical states to the hydrodynamics requirements. It is to be recalled that Q was defined as the effective negative heat of reaction (at 0°K) and is determined from the equilibrium composition.

Consider now a system for which the initial composition and temperature are known. At equilibrium let there be a total of s different molecular specie composed of g individual atomic types. Then, from specie continuity

$$(N_g)_b - (N_g)_a = 0$$

where N_g is the total number of atoms of the gth type. On either side of the wave

$$N_g = \sum_s \alpha_g^s n_s \tag{79}$$

where α_g^s is the number of atoms of the gth type in a molecule of the sth type.

To solve for the equilibrium composition behind a reaction wave, it is first necessary to make a reasonable assumption as to the components which will be present behind the wave and to then write the

appropriate equations for their formation. For each such reaction there exists an equilibrium constant, which depends only on the temperature. Since there are s species composed of g atoms, one needs only s - g equilibrium equations, the remaining equations being the g specie continuity equations. Alternately, depending on the numerical complexity of the calculation, it may be useful to use all s equilibrium relations and utilize the continuity equations as a check.

A general computational procedure would be as follows:

(1) From the measured shock velocity, compute the temperature behind the wave if there was no reaction. ($\beta_a = \beta_b$).

(2) From the knowledge of the type of initial reactants, assume a reasonable value of Δ and correct the temperature to a new value by heat balance (still assuming no reaction).

(3) Calculate the equilibrium at the assumed temperature value.

(4) Compute β_b, Δ, and $\mathcal{M}_b$ corresponding to the first calculated composition.

(5) Compute the pressure ratio from equation (76).

(6) Compute the density ratio from equation (71).

(7) Compute T_b from equation (77).

(8) Compare the calculated temperature from 7 with the value from 2. If significantly different, repeat calculation, using value from 7 as starting point and omiting steps 1 and 2.

Of the several steps in the calculation, the most tedious one is that of computing the equilibrium. This calculation may be performed

by any of several methods and is, in itself an iterative procedure. The selection of the precise calculation technique depends upon the complexity of the reaction scheme and the facility of the calculater in approximation procedures. The development of a general numerical technique is considered beyond the scope of the dissertation and the reader is referred to the thermodynamic literature for resumés of several methods of calculation of complex equilibria.

The rapidity of convergence of the calculation is considerably enhanced if the composition of the material behind the wave is known. In this case, the only purpose of the calculation would be to check if the analyzed product corresponds to a quenched reaction mass or to equilibrium at some other temperature. For this case, the chemical parameters may be directly evaluated from the analysis and the wave velocity checked for agreement with the observed velocity.

For single step reactions, the method is quite rapid, since in this case, a single parameter, the extent of reaction, is sufficient to determine the equilibrium. For example consider the reaction

$$A = B + C$$

with Q of either sign.

Let ξ be the amount of A reacted. At equilibrium the composition will be

$$A = (1 - \xi)\, A_o$$

$$B = \xi\, A_o$$

$$C = \xi\, A_o.$$

For one mole, then the equilibrium relation will be

$$\frac{\xi^2}{1-\xi} = K(T_b) \tag{80}$$

Letting $Q = -\xi\Delta H^o$, then $\Delta = -2\xi\Delta H^o/R_aT_a$. The equation of state for the reaction products is

$$P_b = \rho_b R_o \left(\frac{1-\xi}{m_a} + \frac{\xi}{m_b} + \frac{\xi}{m_c}\right) T_b$$

If the value of ξ is guessed as the first step in the calculation, it is then possible to rapidly calculate the pressure, temperature and density ratios. From the calculated temperature ratio, the equilibrium value of ξ is obtained from (80) and this value compared with the assumed value. If the agreement is not sufficiently good, the calculation is repeated.

An extremely simple case is that of isotope exchange. For these reactions $\Delta \approx 0$ and the gas constants and values of β are simple related. The equilibrium calculation in this case will often reduce to a direct calculation of the temperature from hydrodynamic considerations alone and a separate equilibrium calculation.

In all of these calculations the availability of the thermodynamic data for the specific heats and equilibrium constant at elevated temperatures is usually limited. For the cases where such data is not available, the estimation of these properties is usually best made by the methods of statistical thermodynamics. Furthermore, if the computed temperature (or the assumed temperature) is above about 5000°K, due consideration must be made for the probability of gaseous ionization.

Since the result of ultimate interest in this work is not in the high temperature composition, but in the composition after "quenching"

the reaction, one should consider the calculation of the product produced by cooling from the temperature behind the wave to some lower temperature. Often, this cooling is produced so rapidly that the state of the gas at the lower temperature is one of frozen equilibrium from the conditions behind the wave. As will be shown subsequently, the cooling rate at the termination of the shock tube is sufficiently high that it would be expected that the products would exist in a quenched state.

Let us now consider the problem of the approach to equilibrium behind the shock wave and the case of an insufficiently long section to attain equilibrium. It is to be recalled that the reaction zone is contained by the shock front and the gaseous interface, and that the length of this zone is increasing linearly with time until the initial shock wave reaches the end of the tube. For the tube used in this work, the end consists of an evacuated chamber separated by a thin diaphragm from the test section, and whose volume is about 60 times that of the test section. The moment the diaphragm is ruptured, a rarefaction wave will progress into the reaction zone and quench it. This situation is shown schematically in Fig. 8, which is a wave diagram for this process. As is seen from the diagram, the length of time any particle of gas is maintained at the elevated temperature condition behind the wave will be given by the simultaneous solution of the equation for the particle path and the rarefaction head, or of some arbitrary point on the rarefaction wave. These equations are

$$x - x_o = u_3 \left(t - \frac{x_o}{U} \right)$$

for the particle path and

$$x - L = (u_3 - a_3)\ (t - \frac{L}{U}\ )$$

for the rarefaction. In these equations, the characteristics of the rarefaction wave have been assumed to be straight. Ordinarily, if the reaction zone is not in equilibrium, a temperature gradient within it could cause a variation of the speed of sound in this zone and induce curvature in these characteristics.

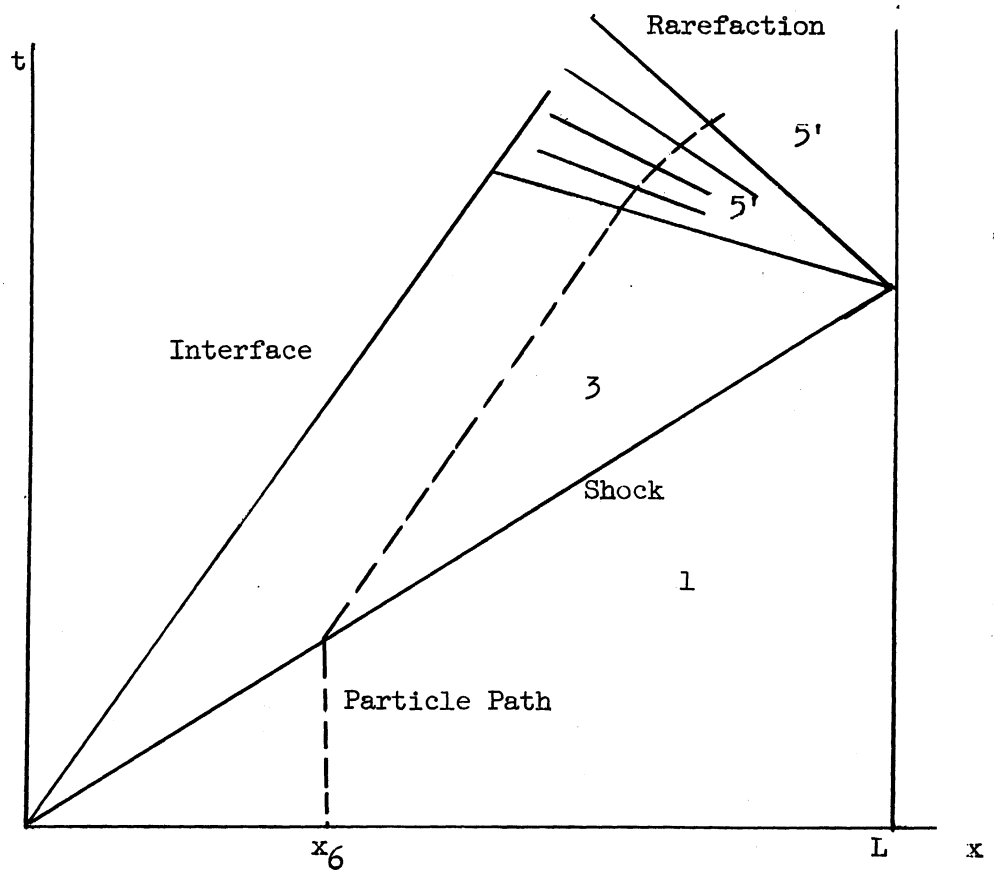

Fig. 8. Wave diagram for interaction of shock wave and evacuated vessel.

Solving for t' the residence time in the wave gives

$$t' = t - \frac{x_o}{U} = (L-x_o)\left[\frac{1}{a_3}\ (1 - \frac{u_3}{U}\ ) + \frac{1}{U}\right] \qquad (81)$$

For a fixed-length shock tube, the reaction products analyzed from the quench chamber will be that composition corresponding to an integrated value over all particle paths. Along a particle path, the rate of reaction will be given by

$$\frac{dA}{dt'} = K_r F(A,B,\ldots) \tag{82}$$

or

$$A - A_o = \oint_o^{f(x_o)} K_r F dt' = A(x_o) \tag{83}$$

where $f(x_o)$ is the residence time t'. The line integral is necessary, since the conversion will depend upon which particle path, i.e., which value of x_o is chosen. Substituting for the value of t in terms of x yields the result

$$A - A_o = \frac{1}{u_s} \int_{x_o}^{f(t')} K_r F \, dx = A(x_o) \tag{84}$$

where f(t') is the distance corresponding to the position coordinate of the intersection of the rarefaction and the particle path. The integral is therefore a function only of x_o. The measured or average composition should be given by

$$\overline{A - A_o} = \frac{1}{u_s} \int_o^L \oint_{x_o}^{f(t')} K_r(T) \, F(A,B,\ldots) \, dx \, d \, dx_o \tag{85}$$

In general, even for the simple case of straight characteristics and no reflected waves considered here, this integral cannot be evaluated in closed form. The inherent difficulty lies in the nonlinear variation of K_r with x. If, however, the variation of K_r through the reaction zone is

small and the composition function F is of zeroth order or is only slightly different than F_o, then (85) may be integrated in closed form. This corresponds to a reaction with very high activation energy. For this case or for $K_r F \approx$ constant, this composition is equivalent to the composition which would be obtained if the reaction had proceeded for the average time given by

$$\overline{t'} = \frac{L}{2}\left[\frac{1}{a_3}\left(1 - \frac{u_3}{U}\right) + \frac{1}{U}\right] \qquad (86)$$

This time average composition is

$$\overline{(A - A_o)}^* = \int_0^{\overline{t'}} K_r F \, dt \qquad (87)$$

Hertzberg and coworkers (19) in considering the specific reaction of $N_2 + O_2$ assume the reaction to take place at some temperature T and space average time $\overline{t'}$. (The nomenclature is the present author's.) The rate equation is then integrated and the experimental values of the reaction composition used to determine the rate constant. This technique is clearly only applicable when the temperature change due to the (adiabatic) reaction is small. In a more general sense the "correct" temperature to be used would be some average value determined from the measured composition.

Far simpler than computing reaction rate constants is the approximate computation of the rates of reaction. Assuming that only the average composition and the wave velocity are known, then the following procedure is suggested to compute the reaction rate.

(1) From the measured composition find the state behind the reaction wave.

(2) Compute u_b.

(3) Find $\overline{t'}$

(4) Divide $\overline{A - A_o}$ by $\overline{t'}$. This is the average reaction rate.

As an example consider a tube 4' long and 1/4 in^2 in area. Let U = 5000 fps, u_3 = 1400 fps, a_3 = 2400 fps, and $\overline{A - A_o}$ = .1 mole fraction product. Computing $\overline{t'}$ gives $\overline{t'} = 10^{-6}$ sec. and therefore the rate is .88 mole/sec - liter. If an average temperature is assumed, the reaction rate constant can be approximated.

E. Shock and Reaction Waves in Real Gases

In this section a few comments will be made on the treatment of the shock front in a real gas. The term real gas will denote one which has molecular transport properties but whose equation of state is still

$$P = \rho RT$$

Becker (1), in 1922, considered a gas undergoing a shock or detonative (exothermic reaction wave) process and assigned to the heat flux vector and pressure tensor the forms

$$\underline{q} = \underline{q}^{(1)} + \ldots \tag{88}$$

$$\tilde{P} = P + P^{(1)} + \ldots \tag{89}$$

where P is the ordinary pressure and $P^{(i)}$ and $q^{(i)}$ are to be defined. The first integrals of the equations of motion for a pure component, now take the form

$$\rho V = A \tag{90}$$

$$\rho V^2 + \tilde{P} = B \tag{91}$$

$$AE + \underline{q} - \tilde{P}V + \frac{AV^2}{2} = 0 \tag{92}$$

Becker (1) and later, Thomas (37), applied what is essentially the Chapman-Enskog technique in the solution of these equations. In this solution, the heat flux vector has the form

$$\underline{q} = -\lambda \frac{dT}{dx} + f\left(\frac{d^nT}{dx^n}, \frac{d^nV}{dx^n}\right) \tag{93}$$

$$P = P - \frac{4}{3}\mu \frac{dV}{dx} + g\left(\frac{d^nV}{dx^n}, \frac{d^nP}{dx^n}\right) \tag{94}$$

Considering only the first term in (93) and the first two terms in (94), yields the equations

$$\rho V^2 + P - \frac{4}{3}\mu \frac{dV}{dx} = B \tag{95}$$

$$\frac{AV^2}{2} + AE - \lambda \frac{dT}{dx} - VP + \frac{4}{3}\mu V \frac{dV}{dx} = C \tag{96}$$

The equation of state may be used to express P as a function of ρ and T, and from thermodynamic considerations for a polytropic gas E may be expressed as a function of T. Becker and Thomas limit their discussion to the case of

$$E = 3/2\ RT$$

that is, a noble gas.

The set of equations (90), (95), (96) and the state equation may be solved for the unknowns ρ, P, T, and V. These equations imply that in a real gas there can be no sharp discontinuity but that the gas passed

from the state (a) in a continuous manner to the state (b). State (b) is only reached asymptotically. Fig. 9 shows the approximate nature of a shock wave in a real gas on a P-x plot.

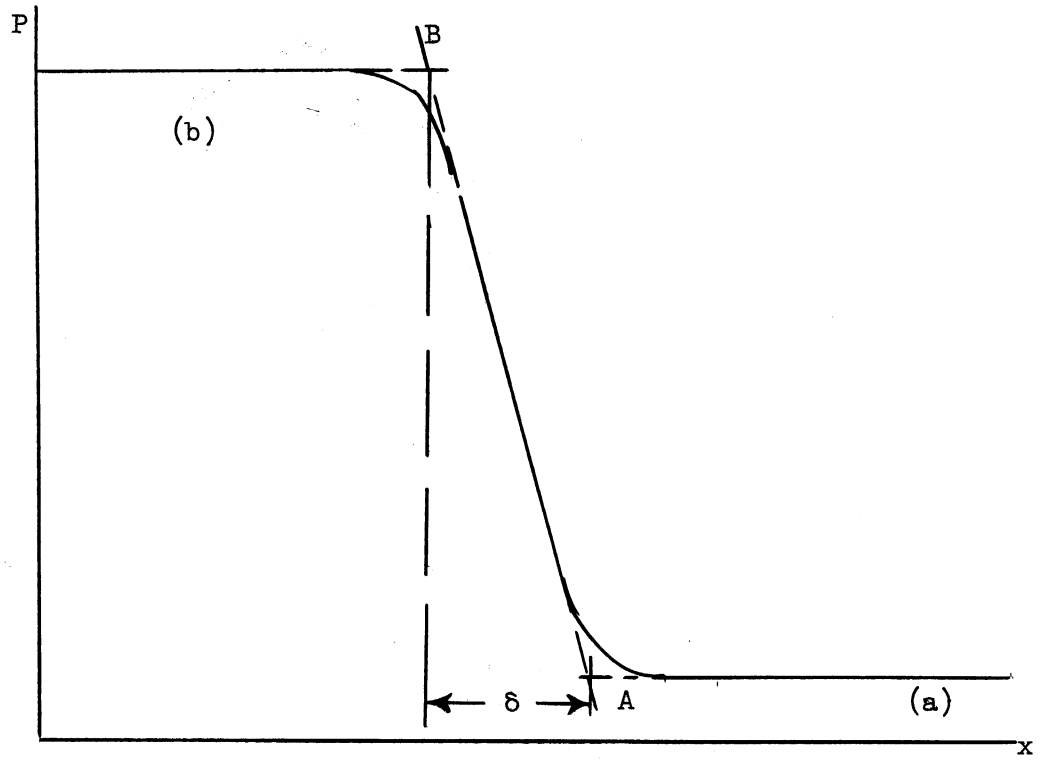

Fig. 9. P-x plot for shock wave in a real gas.

Fig. 9 also shows schematically what is meant by the thickness of a shock wave (δ). This distance is defined as the distance between the points of intersection of the line A-B with the asymptotic values of pressure. The line A-B is drawn as the extension of the nearly straight portion of the curve connecting (a) and (b). δis usually of the order of a few mean free paths.

In view of the last statement, the question can be raised if the equations of change, derived for a continuous medium, may be

applied to processes which occur on a molecular scale. Rigorously, the answer is no, although the results obtained by the continium methods are in reasonable agreement with more exact methods. Mott-Smith (29) have considered a solution for the shock wave based on the application of Boltzmann's equation near the wave. The solution is somewhat intuitive in that he assumes the gas to possess a Maxwellian distribution on each side of the wave and then calculates the transition. Cotter (9) has extended this approach to the case of a chemical reaction and concludes that for common gases the reaction does not occur within the front but is initiated by the wave and proceeds behind it.

Finally, for real gases with internal degrees of freedom the deviation from thermal equilibrium must be considered. This gives rise to the so-called "relaxation effects". By this is meant that the states of the gas as it passes from the initial state (a) to the asymptotic state behind the wave (b) are not states of equipartition of energy. Furthermore, there is a finite time necessary for each of the degrees to reach asymptotic value and these times may be different. Bethe and Teller have treated this problem in an unpublished manuscript (3) and they conclude that for real gases the vibrational states remain excited for a longer period than the translational or rotational states.

The status of the theory of shock waves in real gases is still one of flux and controversy. The previous discussion has been included for the sake of completeness and to indicate some of the methods of approaching this problem. For the case of reaction waves the physical

models available do not permit any quantitative conclusions to be drawn as to the precise method of initiation. The most satisfactory approach seems to follow Eyring and coworkers (15) in considering the state behind the wave to correspond to the asymptotic value and then apply the usual chemical kinetic methods. As is seen from the previous sections, this method has been used in developing the shock tube equations. The inherent difficulty in a more exact approach appears to be a lack of satisfactory physical models.

III. THE EXPERIMENTAL SHOCK TUBE AND ITS OPERATION

A. General Remarks

The equipment used in the experimental portion of the work consisted of a specially designed shock tube and the necessary equipment for the determination of wave velocities. Auxiliary equipment included both a high and low pressure gas mixing and storage system, vacuum pumps, pressure gauges and sampling lines. The dimensions of the reactor section (or test section) of the tube was 1/2" x 1/2" x 4'. At one end of the tube was the high pressure or reservoir section and at the other was the low pressure (or quench) chamber. These various sections were separated by means of diaphragms held on movable slides.

Fig. 10 is a photograph of the shock tube showing some of the essential components as follows:

A. Test section
B. First velocity probe
C. Second velocity probe
D. Product sample bulb
E. Quench chamber
F. Hydraulic pump
G. High pressure chamber (reservoir)
H. Diaphragm.

Fig. 11 is an overall view of the shock tube and all (visible) auxiliaries. These include:

A. Reactant sample bulb
B. Safety shield and mixing console
C. Pulse generator and power supply
D. Electronic chronometer
E. Vacuum pumps.

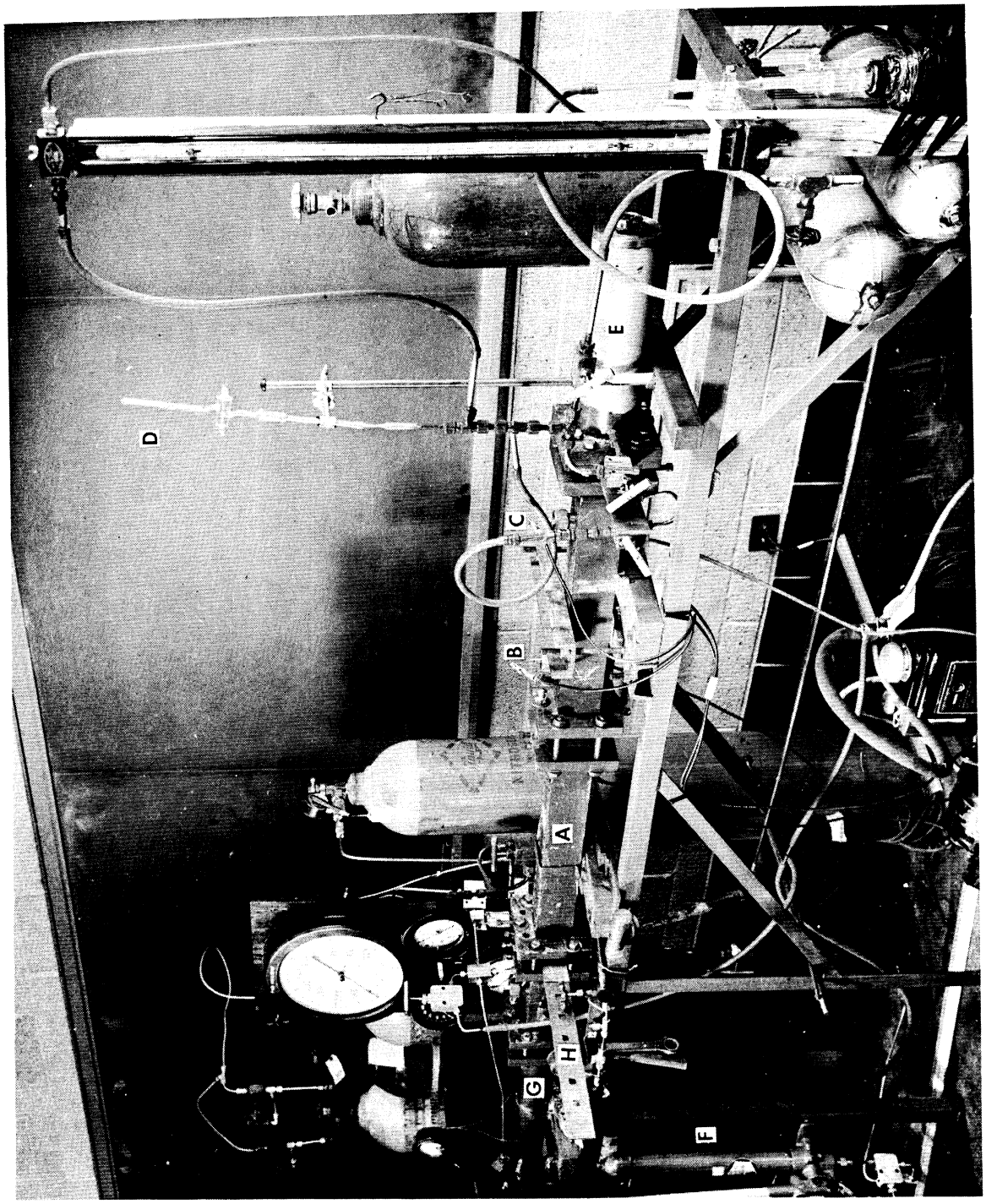

Fig. 10. The shock tube.

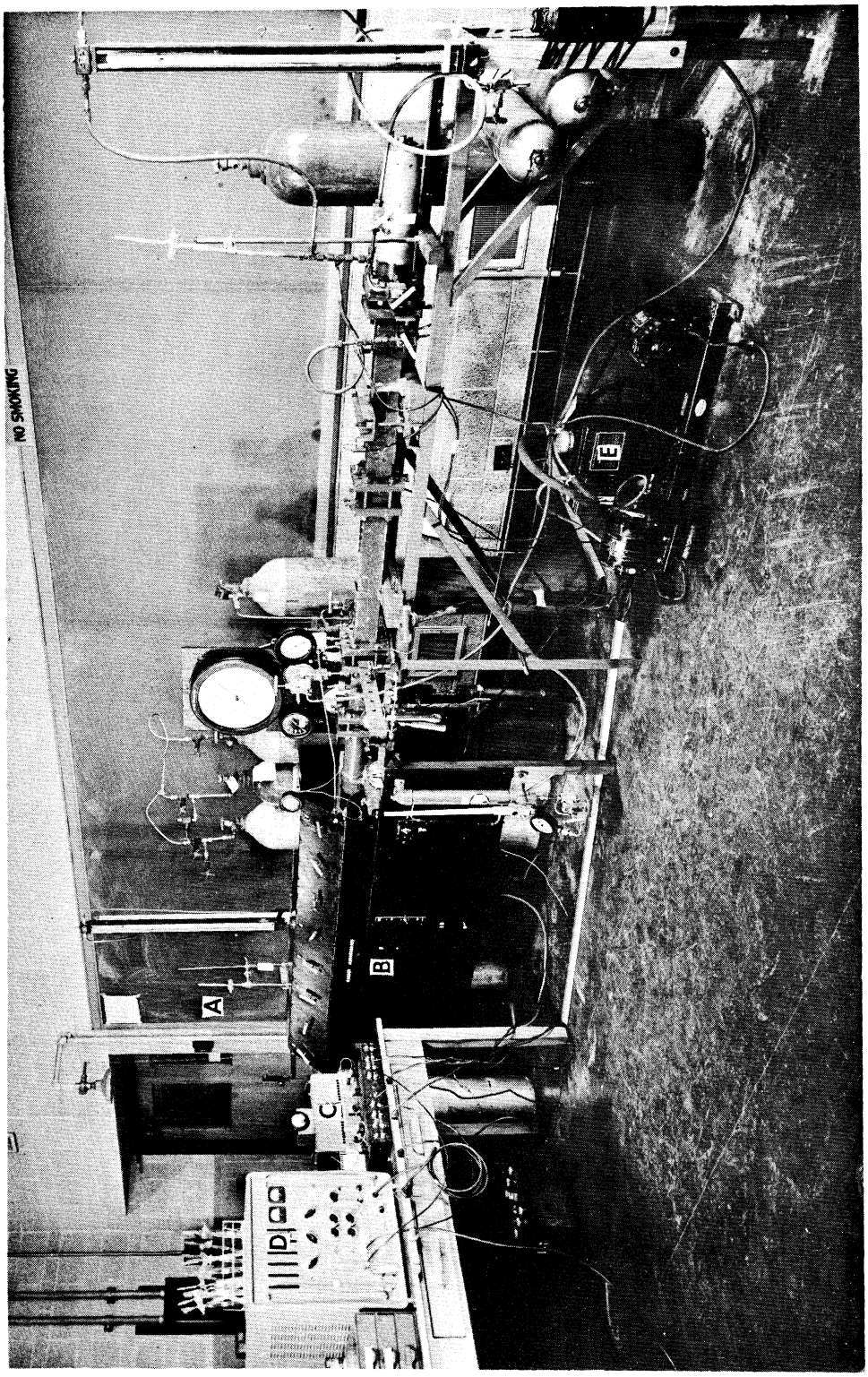

Fig. 11. Overall view of shock tube and auxiliary equipment.

In this equipment, the principle novelty lies in the use of a variable volume reservoir chamber to increase the driver gas pressure and the use of an evacuated quench chamber to freeze the reaction. Provision was made for the introduction of a high pressure glow plug igniter in the reservoir. The entire test section and reservoir were designed to withstand static pressure in excess of 100,000 psi. As an added measure of safety all valves, fittings, and connecting tubing for the test section, reservoir, high pressure storage vessels, and mixing console were of the superpressure type distributed by either Autoclave Engineers of Erie, Pennsylvania or American Instrument Company of Silver Spring, Maryland. Sections of the equipment which operated between atmospheric pressure and 2000 psi were fabricated with commercial valves rated at 4000 psi working pressure or better, Ermeto fittings, and stainless steel or mild steel tubing of similar specifications.

All joints between adjacent sections or on removable components (i.e., velocity probes) were sealed by means of "O" rings or specially designed gaskets.

Calibrated Bourdon tube gauges were used to measure all positive pressures in excess of 30 psia and U-tube manometers were used of pressures below 30 psia.

The choice of the square cross section for the tube was dictated by a desire to increase its versitility and to permit the possible use of optical techniques in the determination of the wave properties. However, these techniques were not used.

The entire tube was constructed of mild steel and the use of this material necessitated periodic dismantling and cleaning. It was felt that the added expense of stainless steel or other materials for the tube could not be justified.

B. Design and Construction of the Shock Tube

In the design of a shock tube, it is required that range of operation of the device be fairly well established. In particular, it is necessary that the minimum velocity in the test section be established and the type of gases to be used in the reservoir and test section be established. For this purpose, the design was based on a minimum Mach number of 4 in the test section. Gases having substantially the same properties as air and hydrogen were selected for the test section and reservoir, respectively.

Denoting L as the length of the test section and Λ as the length of the reservoir, it is first necessary to determine the length ratio L/Λ. This ratio must be such that the gas contained between the shock front and the interface (the hot gas) reaches the end of the test section before the reflected wave from the end of the reservoir can interact with the interface. Using the NACA Tables (46) the pressure ratio across the shock wave is 18.5. Using again the nomenclature of Fig. 3, this is π_{31}. From equation (62), the diaphragm pressure, π_{21}, ratio is 66.5 if $T_1 = T_2$. The velocity behind the shock wave, u_3, is computed from equation (58) and has the value $3.14a_1$. It is possible to find the rarefaction pressure ratio

from π_{31} and π_{21} and it has the value $\pi_{23} = \pi_{24} = 3.6$. The temperature at the foot of the rarefaction is computed from isentropy as $T_4 = T_2(3.6)^{-.286}$ $= .695\ T_2$ and $a_4 = 3.11a_1$, since a_2 has the value $a_2 = \sqrt{14a_1}$ from the problem statement. Since the time required for the interface to reach its end of the tube is $L/3.14a_1$ seconds, the required length Λ may be estimated from the inequality

$$\frac{\Lambda}{\sqrt{14a_1}} + \frac{\Lambda + L}{\left(\frac{dx}{dt}\right)_f} \geq \frac{L}{3.14a_1}$$

where $(dx/dt)_f$ is the final slope of the reflected rarefaction head. This estimate is conservative since the path followed by the rarefaction is as shown by the solid line A-B-C-D--- in Fig. 12. The dashed line is the approximate solution used here and the result is certainly conservative. Computing $(dx/dt)_f$ from equation (57) yields

$$\left(\frac{dx}{dt}\right)_f = u_3 + a_4 = (3.14 + 3.11)\, a_1 = 6.25a_1$$

Solving the inequality gives

$$\frac{L}{\Lambda} \leq 2.84$$

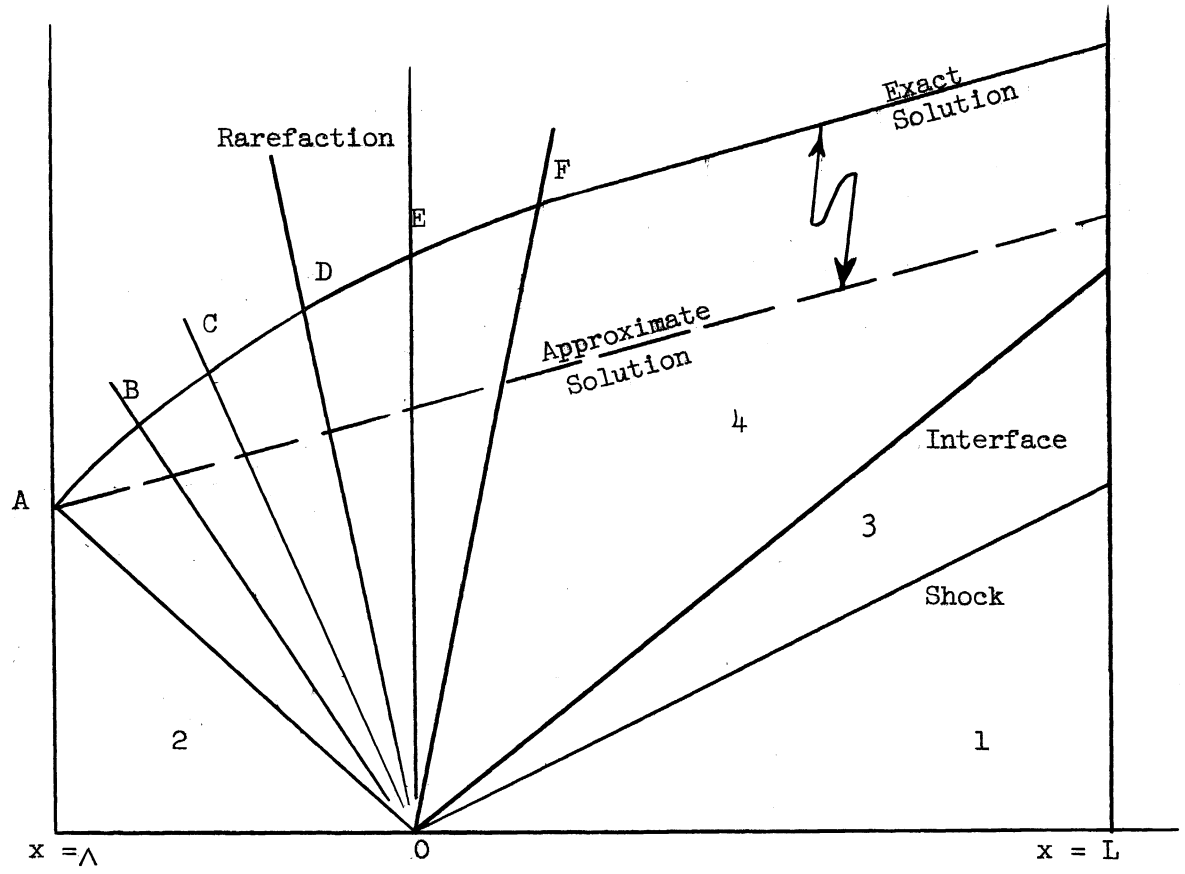

Fig. 12. Wave diagram for determining L/Λ

On the basis of this calculation, the value $L/\Lambda = 2$ was selected for design purposes. It is obvious that for a shock Mach number in excess of 4, the ratio will become large, i.e., design based on $M = 4$ is conservative for $M > 4$.

Let us now consider the termination of the shock wave. The method selected was to allow the incident shock to expand into an evacuated chamber of large volume and area much greater than that of the test section. Physically, this was accomplished by separating the evacuated chamber (quench chamber) from the test section by means of a thin diaphragm. It is necessary, however, to determine the quenching characteristics of this device.

Because of the differences in pressure at the area change, it is true that a rarefaction will be propagated into the hot flow. This rarefaction will be centered and the computation of the cooling rate may be approximated. Again consider a Mach 4 shock in air and a shock tube length of 4'. At the instant the diaphragm is removed, a rarefaction is propagated with a velocity

$$\frac{dx}{dt} = u_3 - a_3.$$

From the previous result u_3 has the value $u_3 = 3.14\ a_1$, and $a_3 = 2.02a_1$, or $dx/dt = 1.12a_1$. By arbitrarily selecting the point on the rarefaction whose pressure is 90 percent of the initial pressure, the value of u_5 is obtained by use of equation (59b):

$$u_{5'} = (2.02 + 02)a_5 = 2.04a_1.$$

At 5' the temperature is $T_{5'} = .97T_3$ or $\Delta T = -.03T_3$. The cooling rate, dT/dt is then

$$\frac{dT}{dt} = \lim_{\substack{\Delta x \to 0 \\ \Delta t \to 0}} \frac{\Delta T}{\Delta x}\frac{\Delta x}{\Delta t} = \left(\frac{u_{5'}+u_4}{2}\right) \lim_{\Delta x \to 0} \frac{\Delta T}{\Delta x}$$

Consider an interval of 10^{-6} second; Δx is computed as $2.03a_1 \times 10^{-6}$ feet or therefore the initial cooling rate,

$$\frac{dT}{dt} = -0.06\ T_1 \times 10^6\ ^\circ K/sec.$$

This rate may not, of course, be sustained, for after 100 microseconds the rate will fall to $-0.06T_1 \times 10^4 ^\circ K/sec$. However, for the selected condition the time interval between the arrival of the shock and the interface at the end of the tube is 128 microseconds. The temperature

drop at the end of this period is estimated as 900°K or the final temperature is 300°K. The quenching action is thus established and the possibility of frozen equilibrium is indicated.

Having established the L/Λ ratio and the termination, the remaining problems were purely mechanical. To avoid excessively large or bulky equipment, L was selected as 4 feet and therefore, Λ became 2 feet. The test section was chosen as 1/2" x 1/2". An overall schematic diagram of the shock tube and gas handling equipment is shown in Fig. 13.

The test sections and the section of the reservoir closest to it were constructed by milling a 1/2" x 1/2" slot in a piece of 1-3/4" x 3" cold rolled steel. In addition two 1/8 x 3/32 slots were milled on either side of the 1/2" x 1/2" slot to accommodate 1/8" round aluminum wire, which was used as a gasket. The upper covers of these "U" shaped channels were 1-1/4" x 3" cold rolled steel. The channels and cover plates were assembled by means of 3/8 - 24 NF Allen head screws located on 1" centers. Two dowel pins were located at the opposite ends of each section. After the initial assembly of the tops and bottoms of the sections, the ends were carefully machined square and finished. For the test sections, the finishing consisted of machining "O" ring grooves, whereas the reservoir had a 2" x 1/4" slot milled on its face and then "O" ring grooves machined in this slot. Figs. 14 and 15 show the method of assembly and the slot and "O" ring groove details. The second section of the reservoir was a tube 3" O.D. with a 33/64" hole reamed in it. One end was finished by machining "O" ring grooves and the other was drilled and reamed for a high

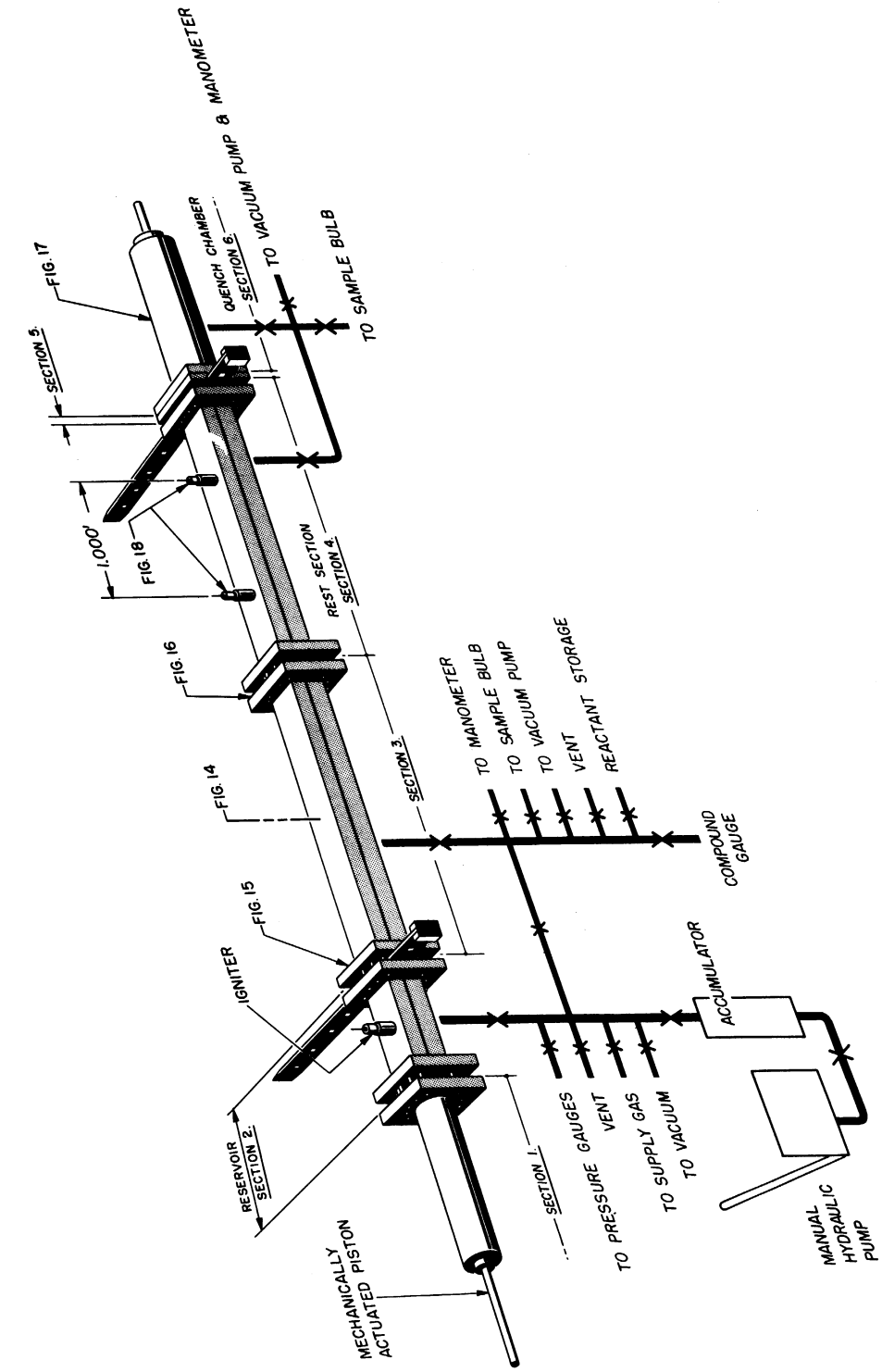

Fig. 13. Diagram of the shock tube and associated lines.

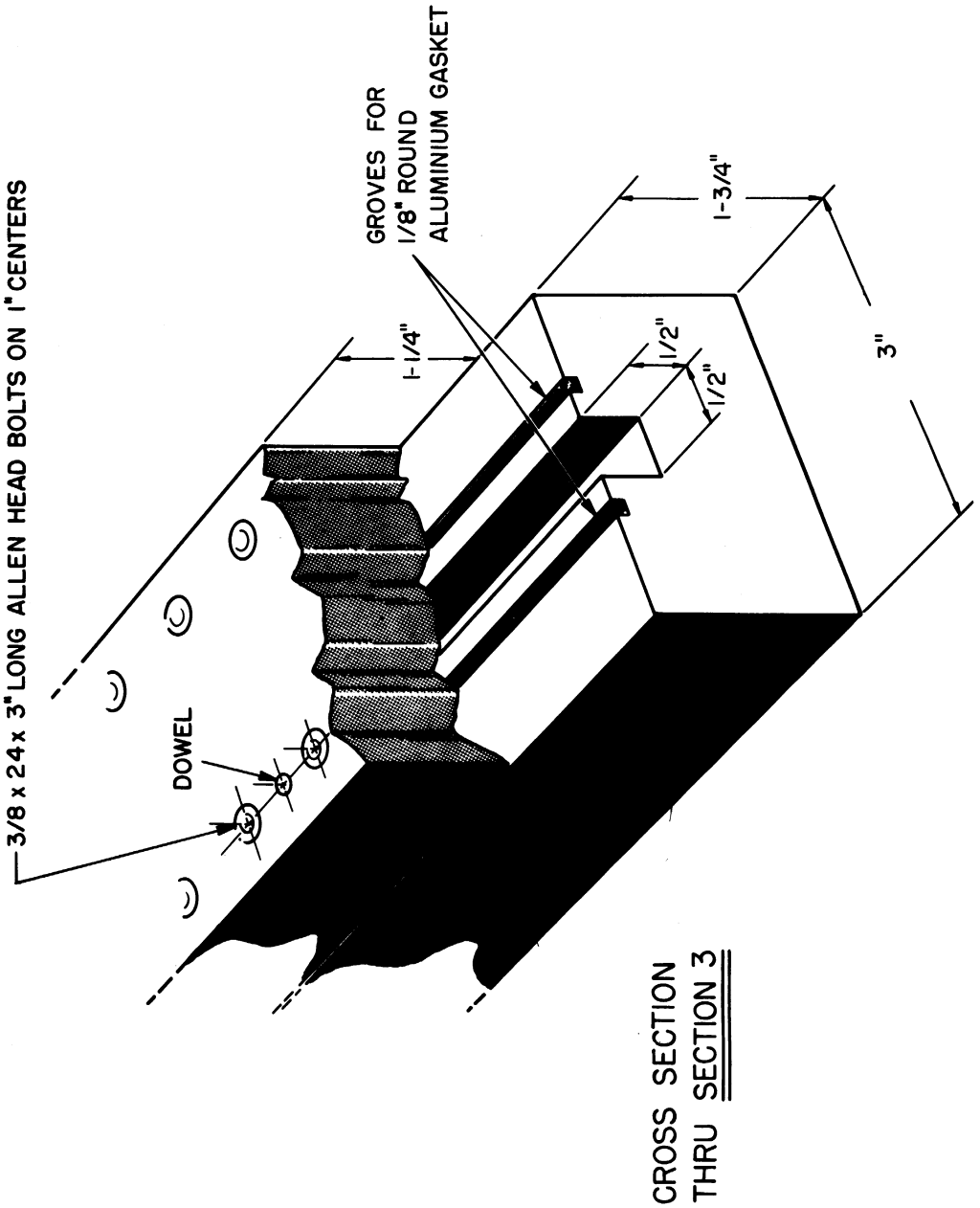

Fig. 14. Method of assembly of test section.

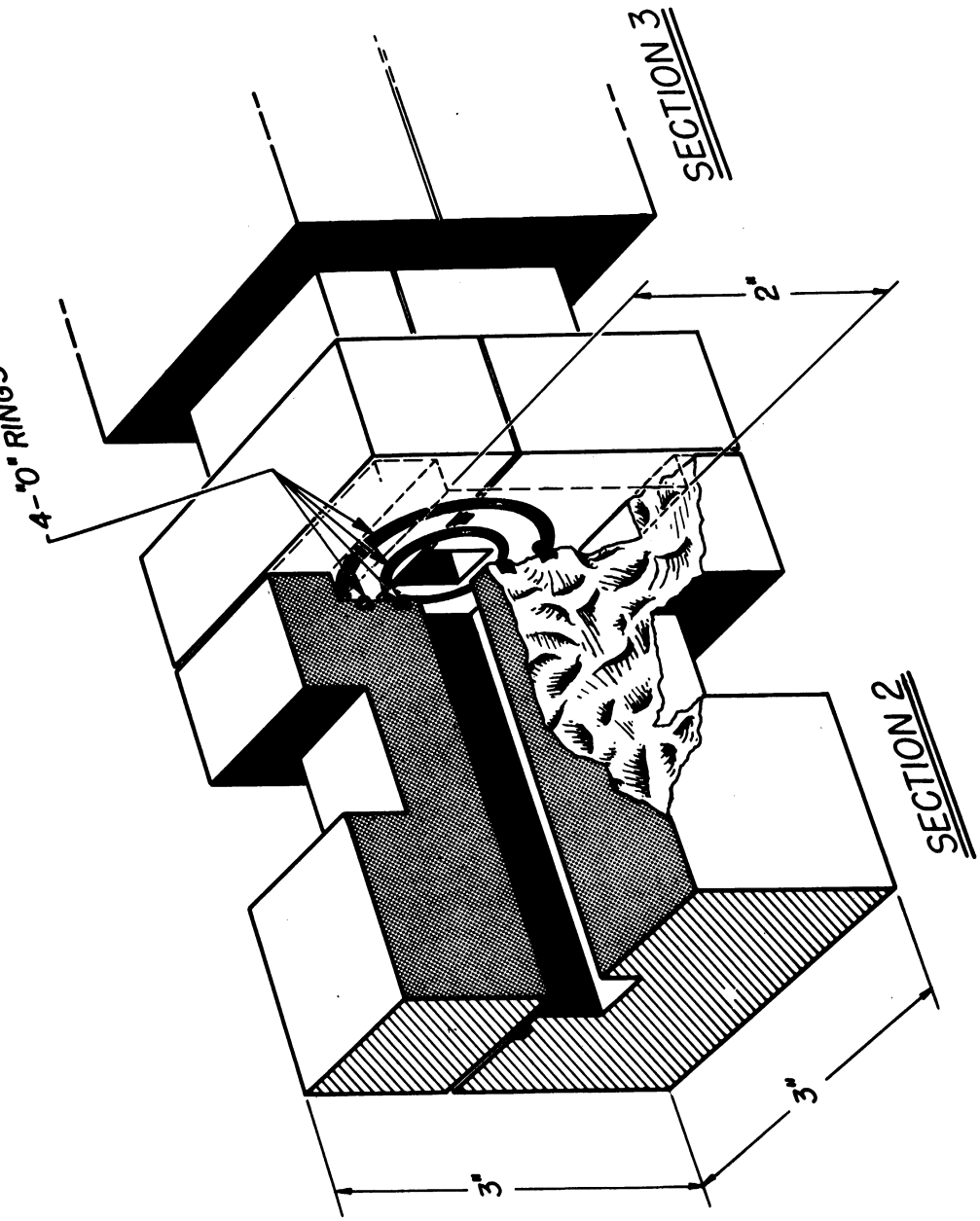

Fig. 15. Slot and "O" ring detail.

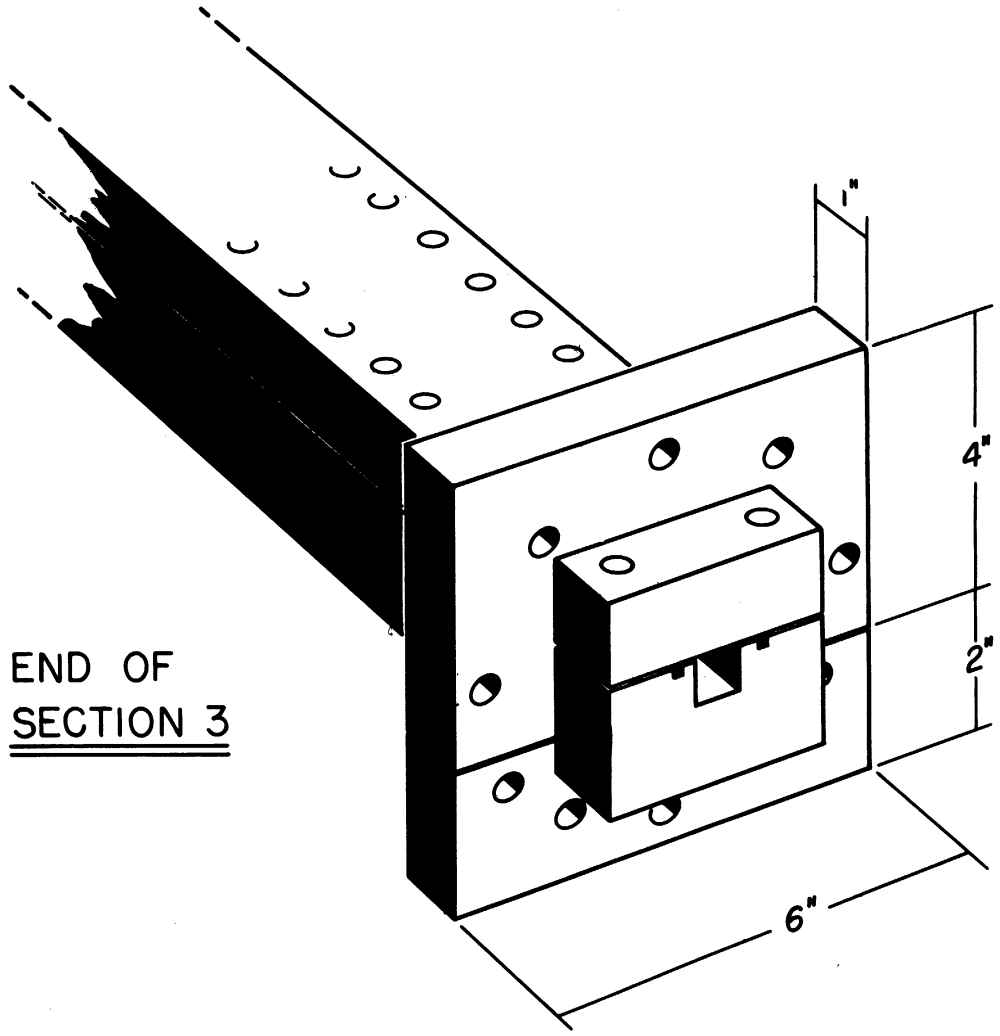

Fig. 16. Detail of flange.

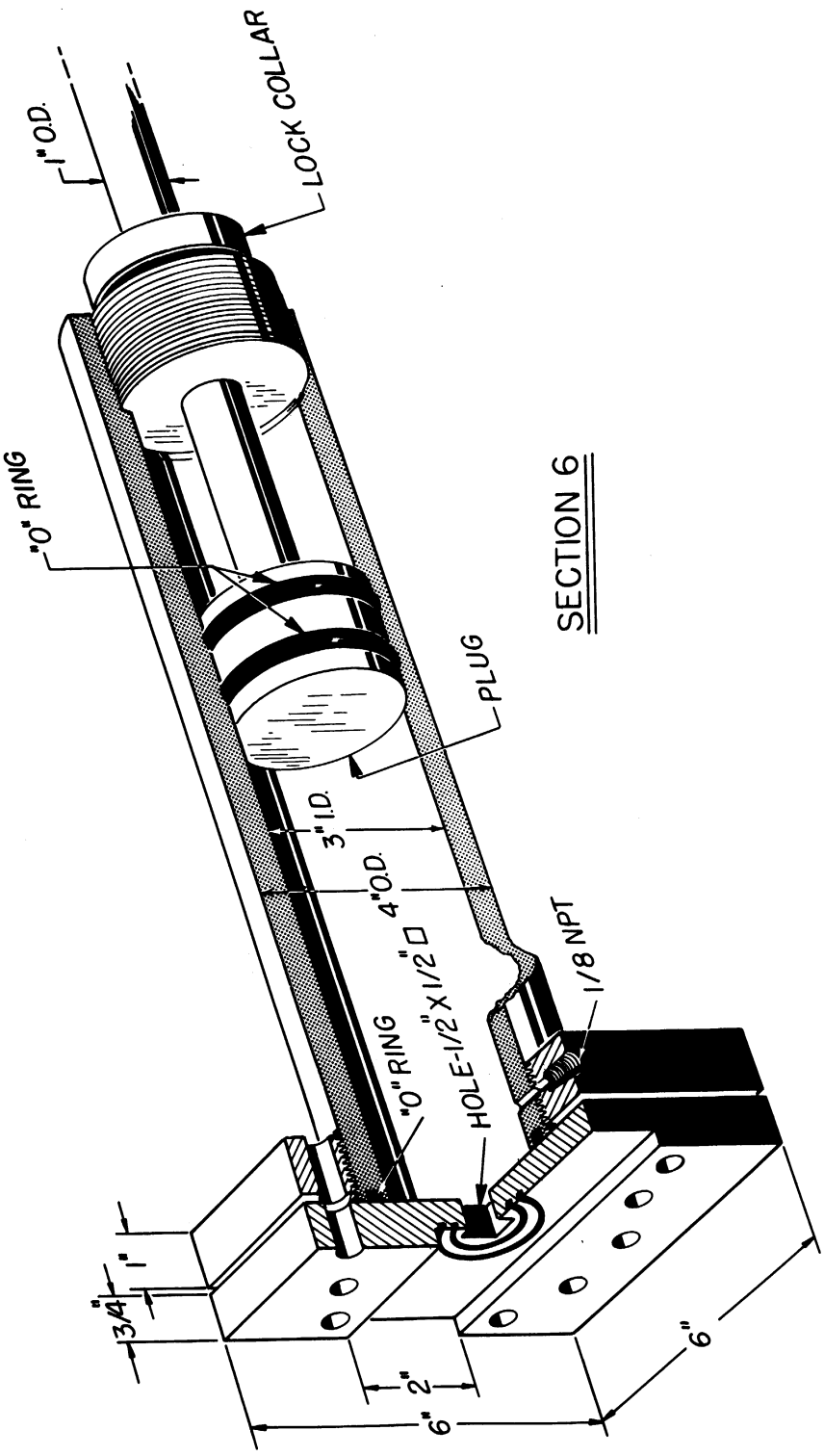

Fig. 17. Schematic of quench chamber.

pressure gasket. This gasket accommodated a .500" drill rod, which served as the piston. The entire assembly was secured by means of split flanges set in grooves milled circumferentially on the sections. In the case of the round sections, the flanges were screwed on and then tack welded. The detail of a flange is shown in Fig. 16. The depth of the slots for the flanges were 1/2".

The quench chamber was fabricated by boring and internal grinding a tube to finished dimensions of 4" O.D. x 3.000" I.D. One end of this tube was threaded internally for 3 1/2 - 12 pitch thread and the other threaded externally for 3-1/2" NPT and had an "O" ring groove machined in it. A plug 2.998" O.D. and grooved for circumferential "O" rings was fabricated, as was a threaded stop collar for the internally threaded end of the tube. Finally, a steel plate 6" x 6" x 1/2" was fabricated to fit between the surge chamber and the end of the test section. This plate had a 1/2" x 1/2" hole punched in its center and a slot 2" wide x 6" long x 1/4" deep milled in its face. This slot was further machined to provide "O" ring grooves, and this formed a section very similar to Fig. 15. The entire surge chamber is shown schematically in Fig. 17.

Finally the necessary openings for the gas lines, velocity probes, and igniter were made and all face joings on the split sections coated with a thin coat of Gyptal Lacquer* and air dried for 24 hours. The basic components were then assembled on an angle iron frame and connected. Alignment was achieved either by means of dowel pins or by passing a

*General Electric Company

1/2" x 1/2" x 6" square brass bar through the open end of the surge chamber down the tube. When aligned, the sections were rigidly clamped to the frame, and the piston on the reservoir connected to an electric motor drive. The plumbing system was installed and a cover made for the reservoir storage vessels and drive mechanism. This cover served both as a safety shield and as a mounting plate for numerous valves.

The diaphragms separating the reservoir and test section were stainless steel, brass or aluminum shim stock up to .042" thick. They were supported in the slots by steel slides in which several 1/2" x 1/2" openings had been punched. Diaphragms to separate the test section from the surge chamber were either .001" steel shim stock or used photographic film about .006" thick. In either case the diaphragm were mechanically weakened before use to insure a minimum of flow disturbance. A slide similar to that used on the high pressure end was used to support these diaphragms.

Connections from the shock tube and its attendant piping to the sample bulbs and vacuum system were made by means of ground glass joints and short length of heavy wall, vacuum type rubber tubing. The sample bulbs themselves were simple glass tubes, sealed at one end with a vacuum stopcock and ground glass joint on the other end. Vacuum was produced by Cenco Megavac Pumps.

C. The Velocity Probes and Timing Circuit

To determine the velocity of the shock waves, it was decided to use simple ionization type detectors and measure the time it took for the wave to travel between two stations whose position is accurately known.

The principle of operation of these devices is quite simple and depends only on the fact that the electrical conductivity behind the shock wave is increased due to the temperature rise. The design of the probes, however, represented more of a challenge since designs which may have offered the best electrical characteristics often did not appear as promising from mechanical considerations. Since the mechanical failure of a probe would represent more of an operating difficulty and hazard than its electrical failure, attention was first directed toward rugged mechanical design. Several designs were actually designed and constructed and all work well mechanically. Except for one design their electrical properties were somewhat variable and eventually all were discarded in favor of the type shown in Fig. 18, which shows the probe and its method of attachment to the tube.

The probe is seen to consist of a body, gland follower, Teflon gasket, and varnish insulated copper wire. On the base of the probe, an "O" ring groove was machined and this served to seal the probe to the wall of the shock tube. By using the copper wire as the central electrode, it was possible to provide extremely close electrical gapping. For the combination of a #18AWG varnish insulated wire, the distance is .0015". By using the moderately heavy 18 gauge wire (.040"), it was quite easy to set the wire flush with the end of the probe. Details of the probe tip and the method of setting the probe in the tube wall are also shown on Fig. 18. The probes were located 1.000 ft. apart.

In operation the probes formed the circuit closing elements in a circuit consisting of a thyratron pulse maker and a Hewlett-Packard Type

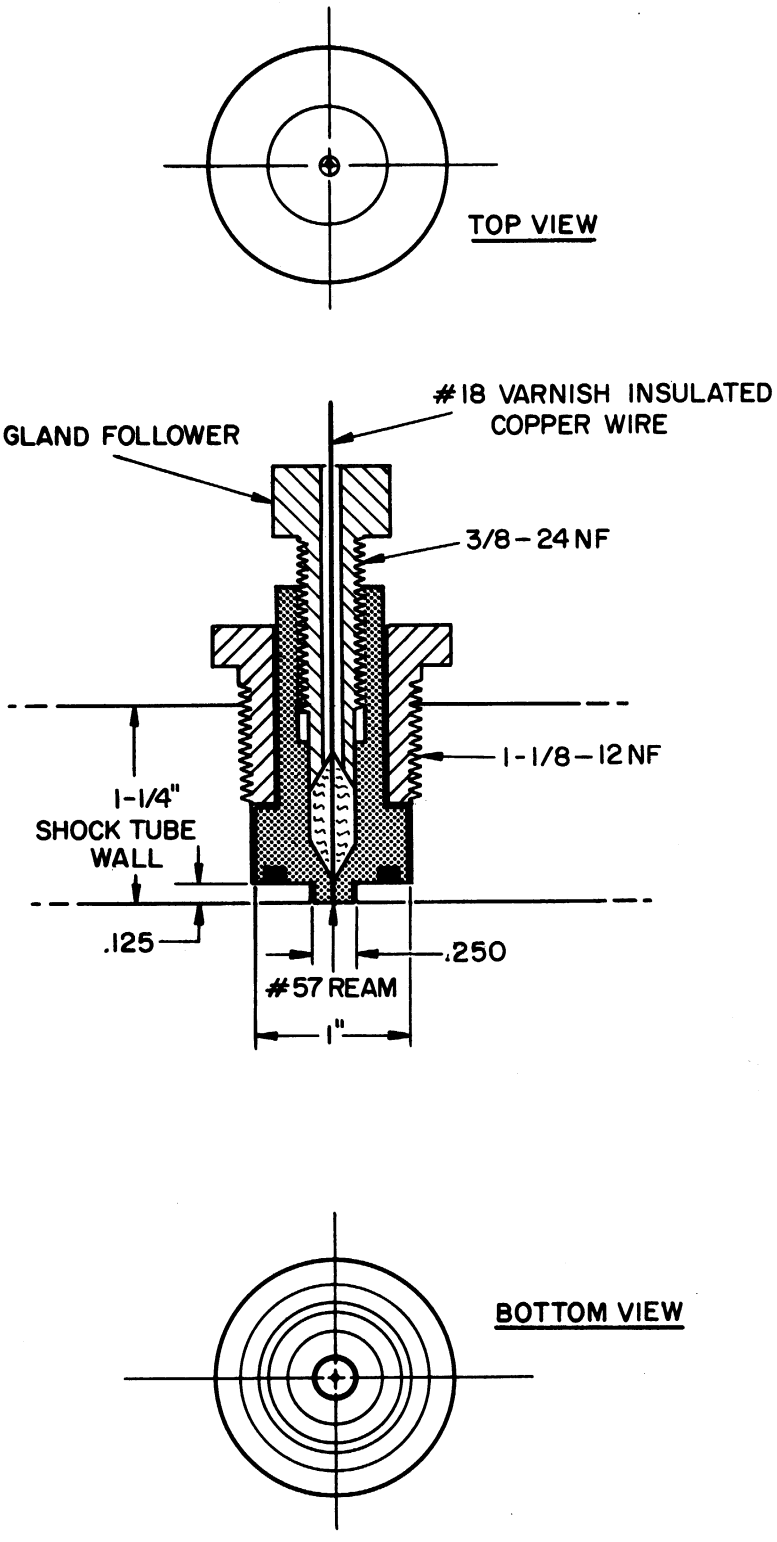

Fig. 18. Schematic of velocity probe assembly.

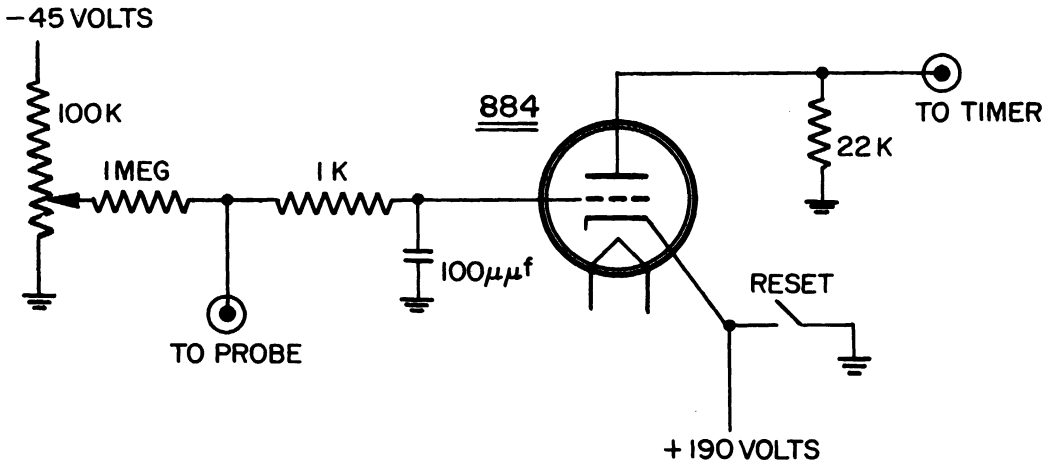

Fig. 19. Pulse maker circuit.

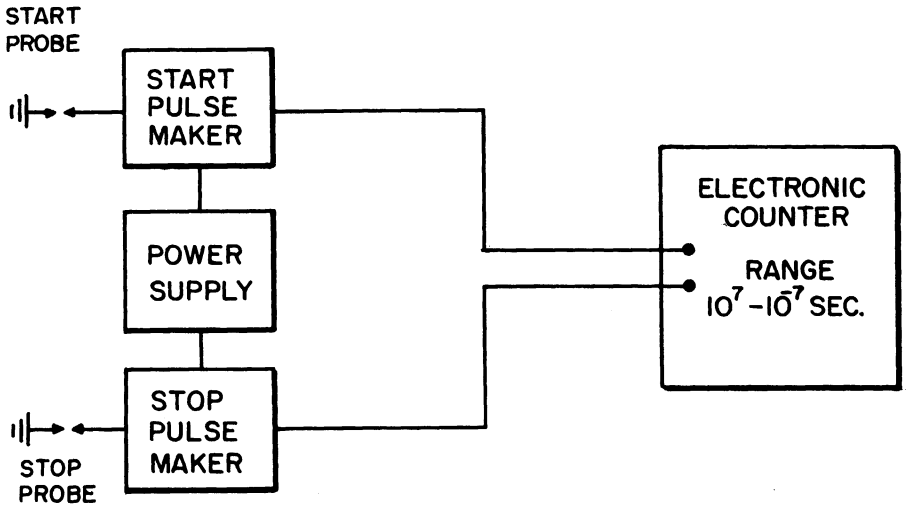

Fig. 20. Block diagram of tuning circuit.

524 electronic counter with a 525B time interval unit. The operation of this circuit is quite simple and is readily seen by referring to Figs. 19 and 20. The probes were first adjusted by means to the 100 K potentiometer until the thyratron just failed to fire. This was usually 12-20 volts bias, depending on the gas in the shock tube, its pressure, history of the probe, etc. When the wave passes the probe, it momentarily causes a current to flow across the probe gap. This lowers the bias potential on the tube, which allows the plate to rise from ground potential to about 190 volts. This voltage is then impressed on the electronic counter, opening its gate circuit and allowing it to count. A similar sequence stops the counter. These pulse makers were calibrated and had a time delay of 0.9 $\pm$ 0.1 microseconds, which is certainly sufficiently accurate. In addition, the electronic counter was calibrated against WWV and the manufacturer's claims for accuracy were verified.

D. Operation of the Shock Tube

In this section the operation and operation characteristics will be described. The principle of operation of the shock tube and the description of operation of the auxiliary components have been covered in previous sections.

Prior to the use of the shock tube for the experimental portion of this work the shock tube, together with the piping and probes, was tested for pressure and vacuum tightness. The former test simply involved replacing the diaphragms with solid steel inserts and applying pressurized gas to the system. A test pressure of 2000 psig was applied to the test section

and the leak rate determined by observing the fall in pressure on a gauge. When properly assembled this rate was less than 5 percent per hour and was considered satisfactory. At pressures below 500 psig, the leak rate was negligible (for positive pressure). The test section and high pressure piping were tested to 7500 psig and a leak rate of about 1 percent per 5 minutes determined. This rate increased considerably with the use of the tube and a periodic replacement of "O" rings at the slotted end was necessary. Losses at all pressures through the piping and reservoir system were negligible. The only appreciable leak in this end was due to aging of the seals in the slotted end of the reservoir.

The entire shock tube and all components (reservoir, test section, surge chamber, gas mixture reservoir, and piping) were vacuum tested collectively and individually. This test involved pumping down to less than 0.1 mm of mercury and determining the leak rate. The leak rate was observed on an ionization type vacuum gauge. The leak rate in the entire system was less than 1 percent per hour and the rates in the gas storage system and test section negligible. The gas sampling bulbs were each tested individually for leakage and were shown to be leak free.

The operation of the tube was quite simple and will be described in the paragraph which follows.

As a first step in the operation of the tube, the proper diaphragms were inserted in the slots and these seals tightened and sample bulbs sealed in their ground glass joints with vacuum grease. Then all sections and inlet lines were evacuated, flushed with the appropriate gas, and

re-evacuated. The reactant gas was then introduced into the test section and sample bulb, and this section isolated. Samples of reactant gas were not taken for every run with the same mixture, but only periodic samples were taken to check the composition.

Next, the reservoir was isolated from the vacuum system and only the surge chamber and product sample bulb remained connected to the vacuum pump. The reservoir gas was then introduced, and depending upon the desired test conditions some variations in technique were employed at this point. If the reservoir gas was to be an inert gas (H_2, He, or N_2) at a pressure below the pressure in the commercial storage tank, it was introduced only into the reservoir section to a pressure 100 psi below the burst pressure of the diaphragm. If the pressure was to be above tank pressure, the gas was introduced into the reservoir and accumulators simultaneously. By means of a sequence of operations involving the hydraulic pump and the piston, the pressure in the reservoir was again raised to within 100 psi of the diaphragm burst pressure and the reservoir isolated. The pressure in the accumulator was then raised to provide gas reserve in case of leaks in the reservoir. Finally, a third method was employed and bears special notice. This technique involved the use of a combustible gas mixture as the driver.

The principle of generating the shock waves by use of a combustible mixture is quite simple and the use of this technique offers several advantages over the previously described method. From Fig. 5 and equation (66), it is seen that by increasing the reservoir to test

section temperature ratio at constant ~~pressure~~ ratio and molecular weight, the strength of the resultant shock wave is increased. However, the main advantage of this method is that it permits much higher pressures to be reached in the reservoir than the purely mechanical system. The final pressure which may be attained by use of this type driver may be calculated assuming adiabatic reaction from the gas mixture composition. The usual values for the ratio of final to initial pressures in a constant volume combustion in the range of 4:1 - 7:1. Thus a final pressure in the test section of 10,000 psi or more can be obtained by use of gas mixtures at pressures not exceeding 2500 psi. Because of the leak characteristic of the reservoir at pressures above 5000 psi, this method offers distinct advantages. As might be expected it does have several drawbacks. These are the possibility of the combustion reaction being detonative, the possibility of corrosive combustion products, and damage to components by the hot gases. Of these three disadvantages, the first was minimized by careful choice of the gas mixture used; the second practically eliminated by use of either H_2-O_2-inert or CO-O_2-inert gas mixtures and carefully flushing the tube after each run. The third problem, that of component failure, was limited to failure of the "O" ring seals after a few runs. Periodic replacement of these units alleviated this problem. Eventually, however, failure of the main seal in the reservoir did occur due to extrusion of the aluminum seal. This would have occurred, however, regardless of the driver system used.

To operate the shock tube with the combustible driver, the following sequence of operations was followed. First, the reservoir and accumulators were evacuated and flushed with helium or nitrogen and re-evacuated. The reservoir was isolated and left under vacuum and the accumulators and hydraulic system filled with inert gas and the gas compressed to about 6000 psi. The choice of inert was dictated by the reactant mixture used. Then the fuel and oxidant were introduced into the reservoir to a predetermined fuel-O_2 ratio. Inert gas was then introduced to give the proper mixture ratio. These ratios were determined from the partial pressures of the components, and the total pressure after mixing was 1-1/2 to 2 times the desired pressure. The mixture was allowed to mix for about 30 minutes. Natural mixing was augmented by slightly compressing and expanding the gas by means of the piston. When the mixing time was completed the pressure in the reservoir was decreased to the desired value by venting excess gas. The valves isolating it were then closed and the tube ready for operation.

The remainder of the operations were the same regardless of the driver technique used. The operation of the electronic instruments was checked, and the surge chamber was isolated from the vacuum pump. Either by increasing the pressure in the reservoir with the piston or by igniting the combustible with a hot wire, the diaphragm was burst and the shock wave propagated through the test section and then quenched in the surge chamber. A sample was taken by isolating the sample line from

the pump and introducing gas directly from the surge chamber into the bulb. The bulb was removed and the entire shock tube vented and purged.

The data recorded in each run was the reactant mixture number, driver composition and pressure, test section pressure, distance between probes and time interval, run number, and sample bulb number. The only experimental difficulty of serious proportion was the occasional failure of the timing system. However, a sufficient number of runs were usually taken at a given set of conditions to rectify the difficulty.

It is seen from the previous discussion that the operation of the shock tube is quite simple. Providing it was not necessary to change any components, a run could be made in about one hour or less.

E. Preparation of Reactant Gases

Reactant gases were prepared by mixing the components to predetermined partial pressures in a previously evacuated stainless steel tank. After introducing the gases into the tank, they were allowed to mix for at least two days before use. In order to increase the molecular weight of the reactant gases, they were often mixed with argon as a diluent. The composition of all feed gases was periodically checked by mass spectroscopic analysis.

F. Analytical Procedures*

All gas samples were analysed by use of a Consolidated Engineering Corporation Type 21-103B mass spectrometer according to the

*The author wishes to extend his gratitude to David M. Brown for his assistance in the analysis of the gas samples.

manufacturer's recommendations for use of this instrument. Basically, this procedure involves standardization of the instrument by means of samples of known composition and then determining the composition of the unknown sample from its spectrum. For the samples of reactant gas, a total analysis was obtained, that is the percentage of each component was determined. For the product gases, this procedure was not employed since in these samples less than 0.5 percent of the mixture was product, the remainder being excess driver gas. The percentage of intermixed driver was not determined; the material balance being obtained from the atomic ratios of the elements in the feed.

IV. EXPERIMENTAL RESULTS

A. The Exchange Reaction of Hydrogen and Deuterium

1. General Remarks

The principle reaction examined in the course of this work was the homogeneous gas phase exchange reaction between hydrogen, mass one (H) and its isotope of mass two (deuterium, D). This reaction proceeds according to the overall stoichiometric equation*

$$H_2 + D \rightleftharpoons 2HD; \Delta H^\circ_{298} = 0.037 \text{ K cal/mole HD}$$

Two distinctly different types of reaction mixtures were used in the study of this reaction; the first was a mixture of D_2, H_2, O_2 and inerts (N_2 and traces of CO_2, A, H_2O, etc.) and the second was a mixture of D_2 and H_2 with or without added argon. Argon was added to increase the molecular weight of the mixture of H_2 and D_2. The addition of oxygen to some of the mixtures was made in order to partially burn some of the H_2 and D_2 and thereby raise the temperature behind the wave. The reaction of $H_2 + D_2 + O_2$ occurs as a detonation and extremely high temperatures may be attained behind these waves. Oxygen was never added in sufficient quantity to oxidize all the hydrogen and deuterium.

*Except where otherwise noted, all thermodynamic data is from U.S. National Bureau of Standards Circular 500 (34).

TABLE II. ANALYSIS OF GASES

	Gas	Supplier	Grade	Composition (Manufacturer's Specification)
Reactants	H_2	Matheson Co., Joliet, Ill.	Electrolytic	99.8% H_2 min., Impurity: H_2O
	D_2	Stuart Oxygen Co. San Francisco, California	Dry	>99.5% D_2; Trace HD
	O_2	Matheson Co., Joliet, Ill.	Dry	99.6% O_2 min.; A, N_2
	A	Matheson Co., Joliet, Ill.	-	99.9% A min.; < .002% H_2; < .002% O_2; N_2
Drivers	N_2	The University of Michigan Plant Department	Water Pumped	99.5% N_2 < .5% O_2; Saturated with H_2O
	He	U. S. Bureau of Mines	Grade A	~100% He; Oil Free, Moisture Free
	CO	Matheson Co., Joliet, Ill.	-	96.8% CO; .36% CO_2; .97% H_2; 1.00% N_2; 0.8% C_nH_{2n+2}

The gas mixtures were prepared from high purity commercial gases whose analyses are given in Table II. The analyses are those supplied by the manufacturers and were not verified. Also included in Table II are the analyses used for driver gases.

To initiate the reaction in the mixtures, the previously outlined procedure was followed. In the case of the H_2-D_2-O_2 mixtures, ignition was easily accomplished with low diaphragm pressures, usually not exceeding 2000 psi.

2. Analysis of Samples

Before describing the experimental results, a few comments will be made on the analysis of feed and product samples. Feed samples were analysed directly by use of an analytical mass spectrometer. Calibration standards of the same quality as the feed components were used and correction made for instrument background. All feed sample material balances closed to within $\pm$ 0.5 mole percent and reproducibility between samples was within $\pm$ 0.5 percent of component. This agreement was considered adequate since the product sample analyses were considerably outside this range and therefore further refinement on feed composition analysis was deemed unnecessary.

The analysis of product samples present a slightly more complex problem. This was due to two factors; one, the unavailability of pure HD for standardization and secondly, the necessity for separating the nearly coincident peaks due to He and D_2 in the mass spectrometer. The latter was accomplished by use of the slowest scan rate available

on the instrument. For the former case, it was necessary to derive the cracking pattern and standardization for HD from the known behavior of D_2 and H_2. The behavior of HD was assumed to be intermediate between that of D_2 and H_2. Its cracking pattern and sensitivity were obtained by linear interpolation between the measured values for H_2 and D_2. Further, for the product analysis only the active constituents were determined (i.e., only H_2, D_2, HD) and therefore these analyses were on an inert free basis. As previously indicated, the material balances in these cases were established by ratios of key components.

The case of the mixtures of H_2-D_2-O_2 represented a unique situation analytically in that the ratio of D/H in the feed was not the same as D/H in the product. Attempts to close the material balances for these samples by analysis of the condensed water product were not successful. This was apparently due to the inability to completely remove all extraneous water traces. The consistency of these data were established by obtaining several samples from runs under similar conditions.

3. Results and Discussion

The experimental results for the H_2-D_2 reaction are presented in Figs. 21 and 22 on which the abscissa is the atomic ratio of deuterium to hydrogen in the product (D/H) and the ordinate is the mole fraction H_2 or HD. Also plotted on these figures are the equilibrium curves corresponding to an equilibrium constant of 4, i.e., as $T \rightarrow \infty$ (See Farkas (16)). The justification for the use of D/H in the product as a significant variable is discussed in the next paragraph.

For the case of no added oxygen the D/H ratio in the feed is of course identical to that in the product. However, when oxygen was added in sufficient quantity to permit the oxidation reaction to occur, the ratio of D/H in the feed was for all runs except one greater than the ratio in the unoxidized product. This result is thermodynamically consistent since the equilibrium constants for the formation of H_2O, DHO, and D_2O are such that

$$K_{H_2O} < K_{DHO} < K_{D_2O} .$$

Since the water formation reaction is extremely rapid at even mildly elevated temperatures, it would be expected that the oxidation equilibria would be established very rapidly and that the excess H_2 and D_2 remaining for the exchange reaction would not be in the original mixture proportion but at some different ratio such that $(D/H)_{original} > (D/H)_{exchange}$. For correlation purposes it has been assumed that $(D/H)_{exchange} = \left(\frac{2D_2+DH}{2H_2+DH}\right)_{product}$. This ratio is equal to (D/H).

In Figs. 21 and 22, the mole fractions of H_2 and HD in the product are shown as functions of D/H. The open circles are the points for the reaction behind the detonation wave and the solid circles are for the runs without oxygen. The most striking feature of these curves is that the points obtained from the reaction with oxygen are all close to the equilibrium line while the points for no added oxygen lie, for the most part, some distance from this line.

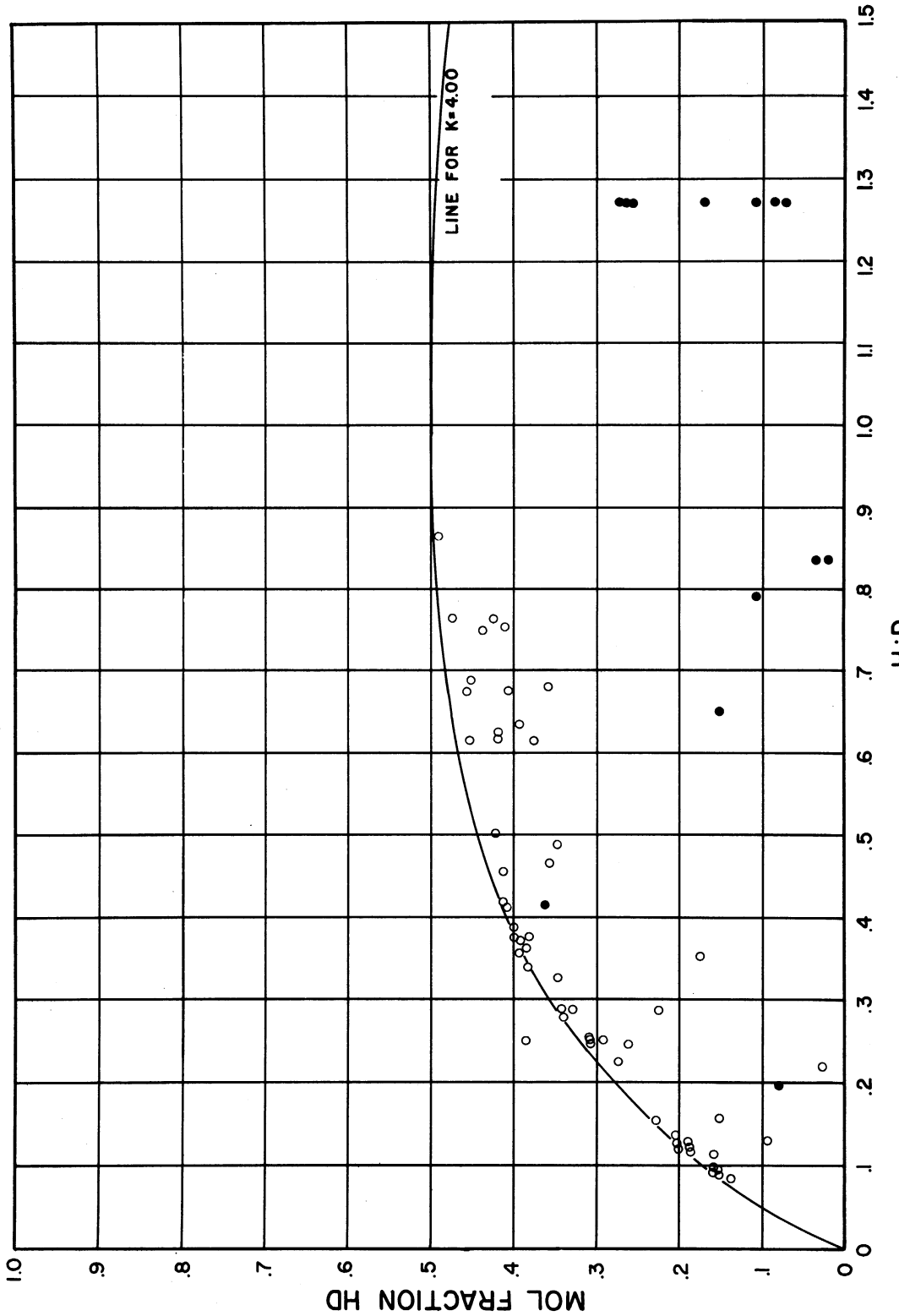

Fig. 21. Mole fraction HD as a function of D/H.

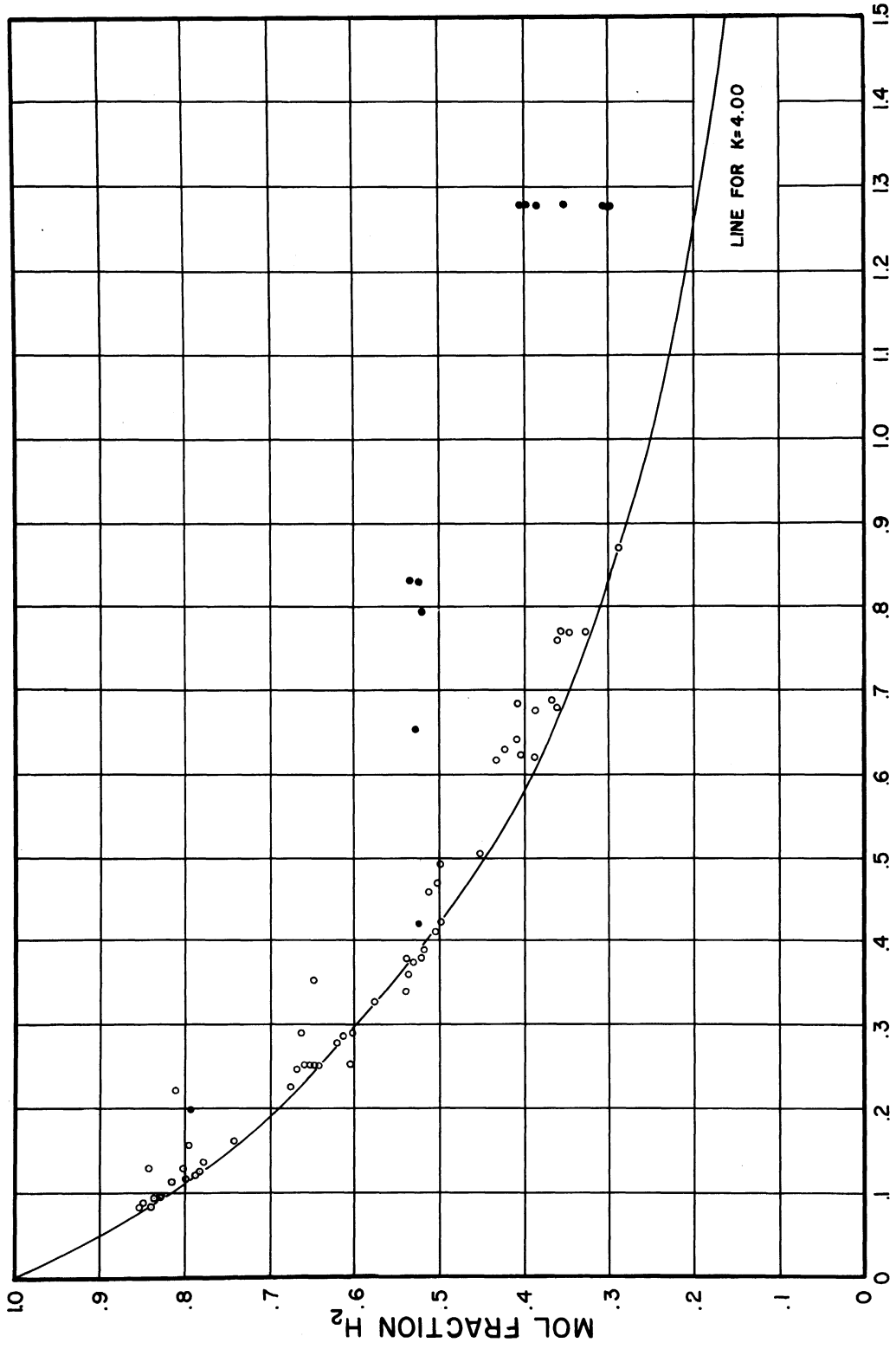

Fig. 22. Mole fraction H_2 as a function of D/H.

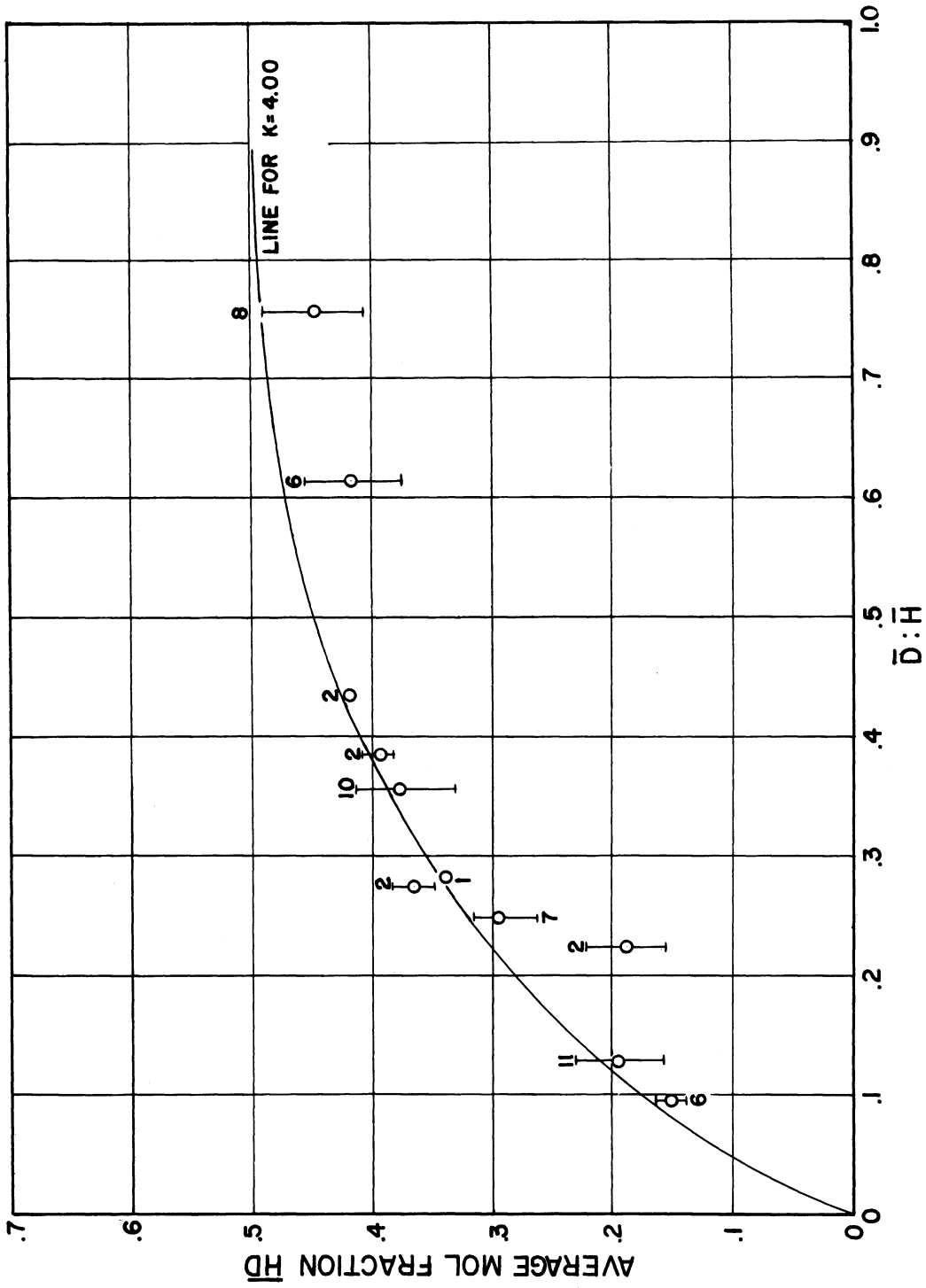

Fig. 25. Average mole fraction HD as a function of $\overline{D}/\overline{H}$.

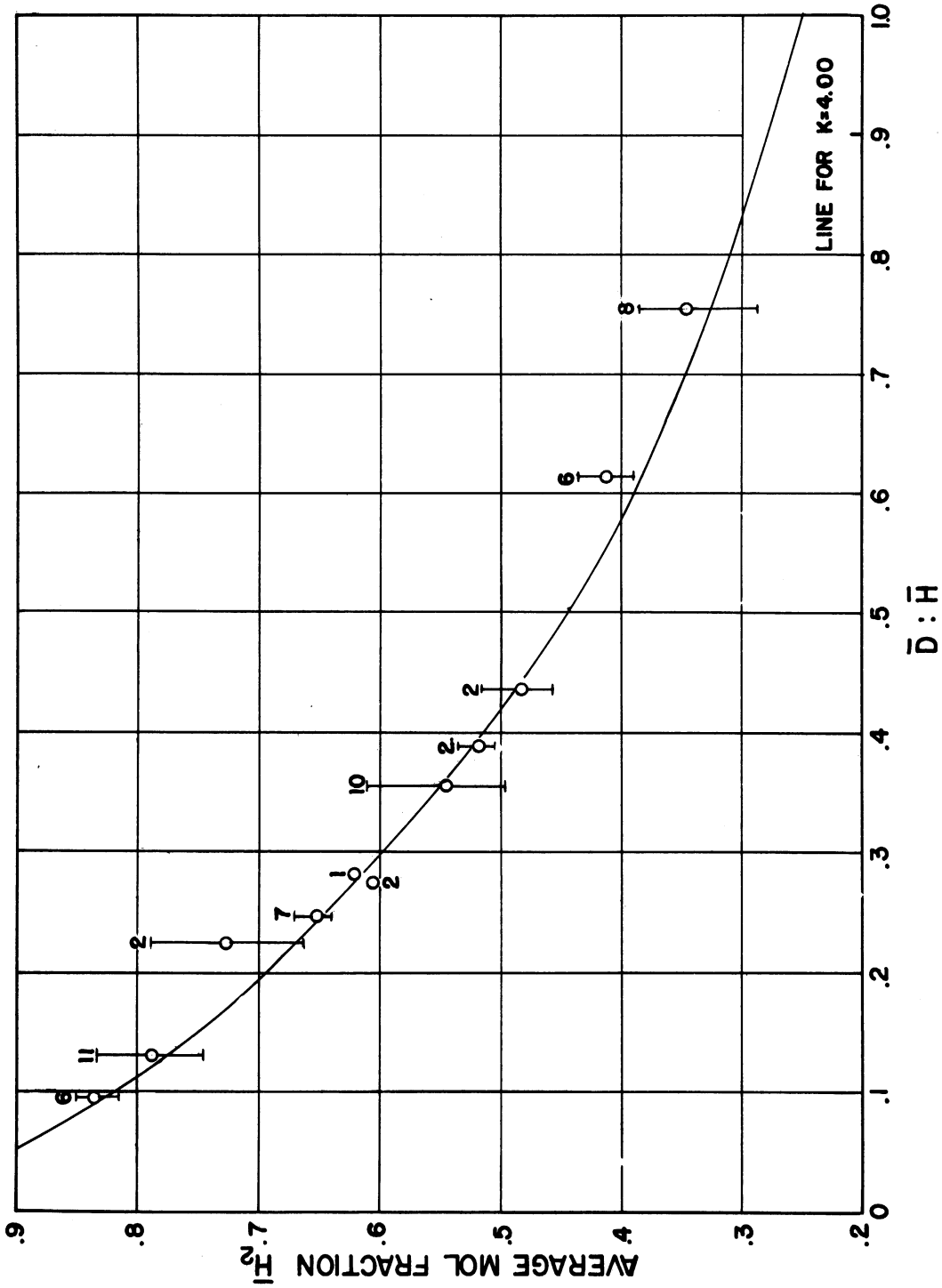

Fig. 24. Average mole fraction H_2 as a function of $\bar{D}/\bar{H}$.

Furthermore, if the data for the case of added oxygen are now grouped by averaging runs made under the same conditions and plotting the average composition vs. the average D/H, the correlation becomes more apparent. The averages used for these correlations which are shown in Figs. 23 and 24 are defined as

$$\overline{H}_2 = \frac{1}{n} \sum H_2$$

$$\overline{HD} = \frac{1}{n} \sum HD$$

and

$$\frac{\overline{H}}{\overline{D}} = \frac{2\overline{D}_2 + \overline{HD}}{2\overline{H}_2 + \overline{HD}}$$

where n is the number of runs and H_2, HD, H/D, the values for the individual runs. The circles represent the average value $\overline{H}_2$ or $\overline{HD}$ and the range of values averaged are shown by the extension lines.

It would appear then that for the reaction of H_2 and D_2 behind a detonation wave equilibrium is very nearly established in the time $\overline{t'}$ defined by equation (86). It is certainly true that if the (space) average composition measured is very near equilibrium then along the first particle paths complete equilibrium should have been attained. It is not possible from these data to make any definitive statements regarding the rate of formation of HD except in the limit sense. Since the velocity of these waves was between 8300 and 11000 feet per second, the time to attain equilibrium may be computed. This time denoted by t_e will be at the most equal to the time it takes for the first particle path to reach the end of the tube or

TABLE III. DATA FOR RUNS AT D/H = 1.28

Feed Composition: .143 H_2; .183 D_2; .674 A

Volume of Test Section: 196.3 cm^3; T_1 = 294°K

Run	Feed Concentration (mole/liter) (10^4) H_2	Feed Concentration (mole/liter) (10^4) D_2	Wave Velocity ft/sec	P_1 in.Hg	P_3 in.Hg	T_3 °k	U_3 ft/sec	a_3 ft/sec	$\bar{t}'$ sec·10^4	Prod. Conc. mole/liter x 10^4	Rate mole/liter-sec	K_{r_1} (10^{-6})
103	3.87	4.95	3600	10	107	990	2637	2210	8.46	.66	.078	.83
109	2.32	2.97	5800	6	168	2170	4330	3240	4.98	.58	.116	1.86
111-112	2.32	2.97	7300	6	264	3170	5500	3960	3.86	1.42	.368	5.95

$$t_e = 8 \times 10^{-4} \text{ sec}$$

Some kinetic data may be obtained from those runs where the deviation from equilibrium is reasonably large. In particular, the six points at D/H = 1.28 are most suited for this purpose since the four usable data points taken from them represent three different operating conditions. These data are tabulated in Table III.

In Table III, the concentrations are computed at T_1, P_1, and the quantities behind the wave are evaluated by the previously developed method. This calculation is shown in Appendix C. The last two columns give the average reaction rate for the exchange reaction

$$H_2 + D_2 \leftrightharpoons 2HD$$

and the reaction rate constant corresponding to the rate if a reversible, second order reaction is assumed. K_{r_1} is evaluated by the relation

$$K_{r_1} = \frac{4.606}{\bar{t}'(A+B)} \log \frac{AB}{AB - \frac{A+B}{2}(HD)}$$

where A, B are the initial concentrations of H_2 and D_2, respectively, and (HD) the final concentration for HD. Concentration units are in mole/liter. This equation is derived in Appendix D.

It is possible to obtain an activation energy by assuming the rate constant obeys the Arrhenius Equation but any value obtained by this technique would be of dubious value since the number of experimental points is small and the assumption of the second order mechanism for the overall reaction is an oversimplification. For completeness, this value of 5 K cal/mole is presented.

TABLE IV. TABLE OF DATA FOR FIGURES 21 AND 22

Run Number	Product Analysis (Mole Fraction) H_2	HD	D_2	D/H
3	.516	.082	.402	.795
8	.531	.033	.439	.833
9	.533	.023	.443	.833
13	.502	.357	.141	.470
15	.796	.158	.051	.158
16	.663	.225	.112	.290
17	.500	.349	.151	.492
18	.365	.454	.481	.690
19	.793	.082	.125	.200
23	.409	.358	.223	.685
25	.454	.423	.123	.505
26	.515	.413	.072	.460
28	.539	.381	.079	.342
30	.504	.408	.088	.412
31	.537	.396	.067	.360
32	.610	.329	.061	.290
33	.516	.346	.079	.330
34	.541	.380	.080	.380
35	.612	.329	.058	.290
36	.520	.400	.076	.390
37	.524	.400	.081	.380
38	.519	.400	.081	.390
39	.540	.386	.074	.364
40	.532	.391	.077	.375
41	.497	.413	.091	.422
43	.603	.346	.056	.292
44	.606	.386	.008	.252
52	.639	.314	.046	.256
53	.679	.274	.047	.226
55	.644	.310	.046	.252
56	.643	.313	.044	.251
57	.653	.293	.054	.252
58	.670	.262	.068	.248
61	.620	.340	.040	.280
65	.836	.153	.010	.095
66	.784	.204	.011	.128
67	.790	.200	.010	.124
69	.799	.188	.013	.120
70	.799	.184	.016	.177
73	.746	.230	.024	.162
74	.777	.203	.020	.138
75	.790	.189	.021	.130

TABLE IV (Continued)

Run Number	Product Analysis (Mole Fraction) H_2	HD	D_2	D/H
76	.853	.139	.009	.085
77	.827	.161	.011	.100
78	.832	.157	.011	.098
79	.850	.136	.014	.089
80	.839	.151	.001	.083
81	.817	.159	.024	.115
84	.365	.458	.177	.690
85	.361	.411	.278	.760
86	.352	.426	.221	.770
87	.326	.475	.199	.770
88	.288	.492	.219	.870
90	.350	.438	.211	.760
91	.386	.406	.211	.680
94	.411	.396	.193	.642
95	.434	.375	.191	.617
96	.425	.421	.154	.629
97	.389	.455	.154	.619
98	.404	.422	.173	.624
103	.401	.075	.524	1.28
104	.305	.267	.428	1.28
105	.396	.085	.518	1.28
109	.384	.110	.507	1.28
110	.353	.171	.476	1.28
111	.303	.269	.427	1.28
112	.302	.272	.425	1.28

The normally accepted mechanism is a chain reaction given by

$$H_2 \rightleftharpoons 2H$$

$$D_2 \rightleftharpoons 2D$$

$$H_2 + D \rightleftharpoons DH + H$$

$$D_2 + H \rightleftharpoons DH + D$$

$$H + D \rightleftharpoons HD.$$

This mechanism was proposed by A. and L. Farkas (16, 17), and has been fairly well established by them and more recently by Van Meerssche (39). The development of a rate equation based on the chain mechanism is possible only if information on the elementary steps can be calculated from a theoretical basis or deduced experimentally. This added refinement is not necessary in this work since only overall rates are desired. The rate constants evaluated from these data are consistent with the time needed to establish equilibrium in the runs with oxygen, if the rate constant is adjusted to the temperature behind these waves.

These results appear to be consistent with the Farkas mechanism for the exchange reaction. In this scheme the rate is controlled by the atomic concentration of H and D, and it would be expected that any technique which yields relatively large quantities of the atoms would give an increased rate of reaction. This is further verified by the fact that at lower temperatures the exchange reaction proceeds only with the presence of a catalyst, and particularly catalysts such as Ni, Pt or other hydrogenation catalysts. Without catalysis, the reaction is

negligibly slow, as demonstrated by the fact that H_2-D_2 mixtures are stable at room temperature.

B. Preliminary Experiments on the Systems H_2-CO_2 and H_2-N_2.

A few preliminary runs were made to examine the reactions

$$H_2 + CO_2 \rightleftharpoons CO + H_2O$$

and

$$N_2 + 3H_2 \rightleftharpoons 2NH_3$$

behind shock waves. With the former system, two runs were made at diaphragm pressure ratios of about 2400; but it was not possible to satisfactorily resolve the product in the analytical mass spectrograph and the shock tube was at a point of incipient failure. No data were obtained with this system.

For the ammonia synthesis reaction, several runs were made in a mixture of N_2-H_2-A at an average velocity of 10,000 ft/sec, very nearly. Again analytical difficulties prevented a quantitative evaluation of the product, although in this case some qualitative observations could be made. The difficulty was due to the inability to completely remove all traces of water from the gases and the instrument and the small total quantity of product present. In particular, water contributes a strong mass peak at the same point as ammonia, and it was not possible to resolve these materials. However, by calibration of the instrument with water the normal ratio of mass 17 to mass 18 was determined and any increase in this ratio in a product sample attributed to

ammonia. It is probable that not more than 2 percent of the hydrogen was converted to ammonia and it can only be qualitatively stated that any product was formed. The evidence is presumptive rather than conclusive.

V. CONCLUSIONS

It may be concluded on the basis of the information obtained in the course of this work that shock waves and hydrodynamically similar phenomena initiate high temperature gaseous reactions. The temperatures which are obtained by the use of shock tube techniques exceed those which are possible in ordinary laboratory systems. Further, it is possible to obtain average rate data for reactions occurring in a shock tube from analysis of the reaction products and the application of the hydrodynamic principles governing the flow in a shock tube. The accuracy of such data is considerably enhanced by operation of the tube in such a fashion that the states of the gases on each side of the wave are nearly the same. It would appear that rates reactions which require gaseous dissociation as a first step are greatly accelerated by initiating the reaction with a strong shock wave since high levels of dissociation may be rapidly achieved.

Finally by application of the equations governing the flow in a shock tube and from rate data obtained in a small laboratory tube, it should be possible to design a device through which reactants will flow on a nearly continuous basis and have the reaction initiated by periodically propagated shock waves.

From theoretical consideration it was demonstrated that shock induced chemical reactions fall into two distinct classes, depending

upon the sign of the heat of reaction. For the endothermic reaction, the extent of reaction is limited by the shock strength and for the exothermic reaction, the extent of reaction is not limited from hydrodynamic considerations.

APPENDICES

APPENDIX A

DERIVATION OF SHOCK WAVE EQUATIONS

DERIVATION OF SHOCK WAVE EQUATIONS

Consider a tube of constant cross sectional area as shown in Fig. A-1. Let the subscript a refer to condition ahead of the wave and b to those behind the wave. The wave velocity will be denoted by U and the velocities ahead of and behind the wave by u_a and u_b, respectively. Velocities will be considered positive to the right.

Referring to all velocities relative to the wave yields

$$V_a = u_a - U \tag{A.1}$$

$$V_b = u_b - U \tag{A.2}$$

and by the jump equations (conservation equations)

$$\rho_a V_a = \rho_b V_b \tag{A.3}$$

$$P_a + \rho_a V_a^2 = P_b + \rho_b V_b^2 \tag{A.4}$$

$$\frac{1}{2} V_a^2 + H_a = \frac{1}{2} V_b^2 + H_b = H_o \tag{A.5}$$

From A.3 and A.4

$$P_a - P_b = \rho_a V_a (V_a - V_b) \tag{A.6}$$

and from A.5

$$\frac{\gamma}{\gamma-1} \frac{P_o}{\rho_o} = \frac{1}{2} V_a^2 + \frac{\gamma}{\gamma-1} \frac{P_a}{\rho_a} = \frac{1}{2} V_b^2 + \frac{\gamma}{\gamma-1} \frac{P_b}{\rho_o} \tag{A.7}$$

or

$$\frac{1}{\gamma-1} a_o^2 = \frac{V_a^2}{2} + \frac{\gamma}{\gamma-1} \frac{P_a}{\rho_a} = \frac{V_b^2}{2} + \frac{\gamma}{\gamma-1} \frac{P_b}{\rho_b} \tag{A.8}$$

From A.6

$$\frac{P_a - P_b}{\rho_a V_a} = V_b - V_a = \frac{P_a}{\rho_a V_a} - \frac{P_b}{\rho_a V_a} \tag{A.9}$$

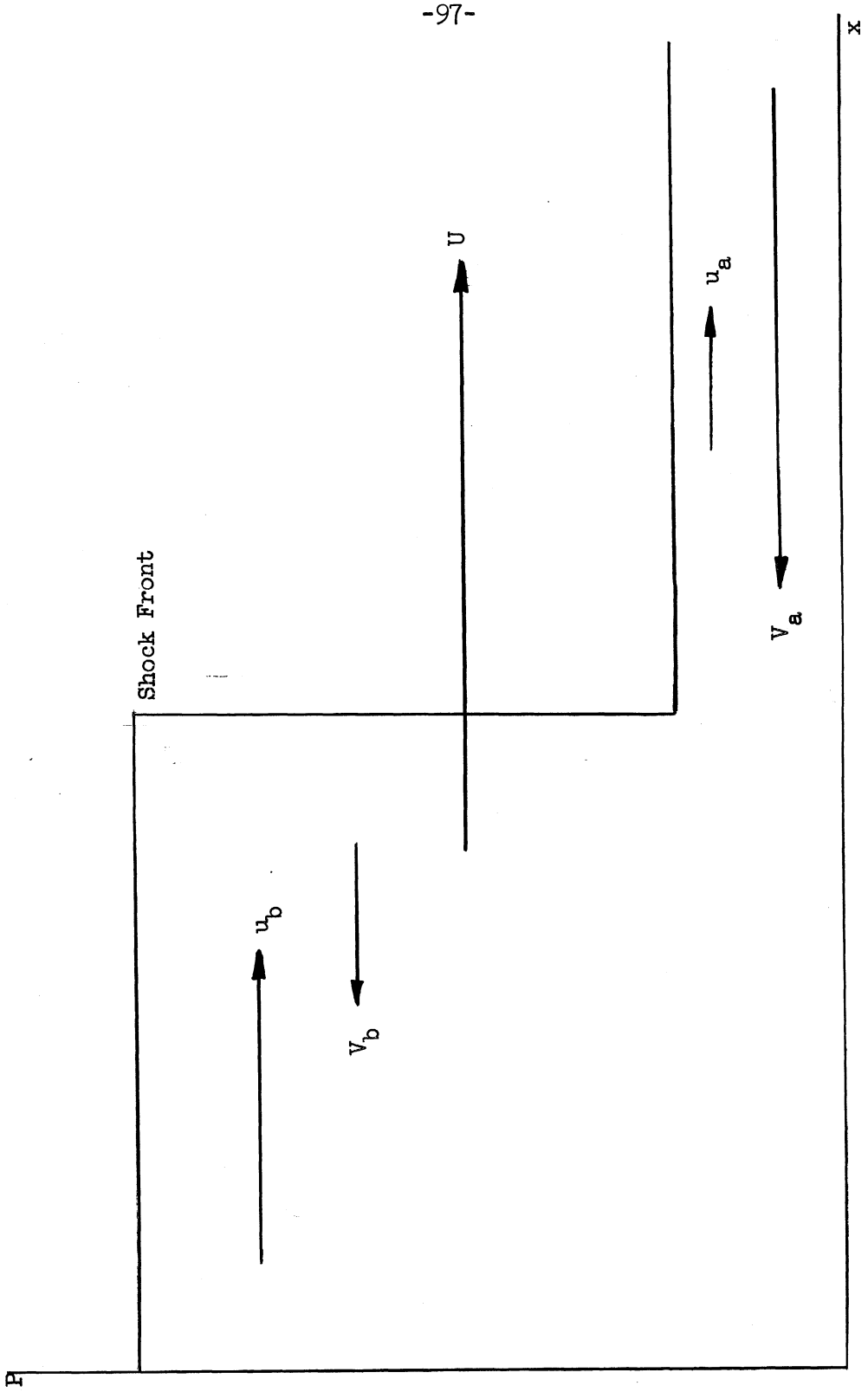

Fig. A-1. Notation for Shock Wave

Dividing A.8 by V_a and V_b, respectively, gives the results

$$\frac{1}{\gamma}\frac{a_o^2}{V_a} - \left(\frac{\gamma-1}{2\gamma}\right) V_a = \frac{P_a}{\rho_a V_a} \tag{A.10a}$$

$$\frac{1}{\gamma}\frac{a_o^2}{V_b} - \left(\frac{\gamma-1}{2\gamma}\right) V_b = \frac{P_b}{\rho_b V_b} \tag{A.10b}$$

which may be subtracted to yield

$$(V_a - V_b) = \frac{a_o^2}{\gamma}\left(\frac{1}{V_b} - \frac{1}{V_a}\right) + \frac{\gamma+1}{2\gamma}(V_a - V_b) \tag{A.11}$$

Rearrangement of A.11 gives

$$0 = \frac{a_o^2}{\gamma}\left(\frac{V_a - V_b}{V_a V_b}\right) - \frac{\gamma+1}{2\gamma}(V_a - V_b) \tag{A.12}$$

or

$$(V_a - V_b)\left[\frac{a_o^2}{\gamma}\frac{1}{V_a V_b} - \frac{\gamma+1}{2\gamma}\right] = 0 \tag{A.13}$$

In A.13 either $V_a = V_b$ or

$$\frac{a_o^2}{\gamma}\frac{1}{V_a V_b} - \frac{\gamma+1}{2\gamma} = 0 \tag{A.14}$$

The former case is trivial (no wave) and consideration of A.13 gives the result

$$V_a V_b = \frac{2a_o^2}{\gamma+1} \tag{A.15}$$

Multiplying A.15 by $a_a a_b / a_a a_b$ and introducing the Mach number gives

$$\frac{a_a M_a a_b M_b}{a_o^2} = \frac{2}{\gamma + 1} \tag{A.16}$$

But from the energy equation, A.5

$$\frac{a}{a_o} = \left(1 + \frac{\gamma-1}{2} M^2\right)^{1/2}$$

which upon substituting into A.16 gives

$$\frac{M_b^2}{1 + \frac{\gamma-1}{2} M_b^2} = \left(\frac{2}{\gamma+1}\right)^{1/2} \left(\frac{1 + \frac{\gamma-1}{2} M_a^2}{M_a^2}\right) \tag{A.17}$$

which reduces to

$$M_b^2 = \left(\frac{1 + \frac{\gamma-1}{2} M_a^2}{\gamma M_a^2 - \frac{\gamma-1}{2}}\right) \tag{A.18}$$

From A.6

$$\frac{P_b}{P_a} = 1 - \frac{\rho_a}{P_a} (V_a V_b - V_a^2) \tag{A.19}$$

which after multiplying and dividing by γ and combining with A.14 gives

$$\frac{P_b}{P_a} = 1 + \gamma \left(M_a^2 - \frac{2a_o^2}{a_a^2 (\gamma+1)}\right) \tag{A.20}$$

which reduces to

$$\frac{P_2}{P_1} = \frac{2\gamma}{\gamma+1} M_a^2 - \frac{\gamma-1}{\gamma+1} \tag{A.21}$$

if the energy equation introduced to eliminate a_o/a_a.

From A.3 and A.4 one has

$$V_b^2 = \frac{\rho_a}{\rho_b} \left(\frac{P_b - P_a}{\rho_b - \rho_a}\right) \tag{A.22}$$

$$V_a^2 = \frac{\rho_b}{\rho_a} \left(\frac{P_b - P_a}{\rho_b - \rho_a}\right) \tag{A.23}$$

which, when substituted into A.5, gives

$$H_b - H_a = \frac{1}{2} \left(\frac{1}{\rho_b} + \frac{1}{\rho_a}\right) (P_b - P_a) \tag{A.24}$$

which is known as the Hugoniot relation. For polytropic gases

$$H = \frac{\gamma}{\gamma - 1} \frac{P}{\rho}$$

and therefore

$$\frac{\rho_b}{\rho_a} = \frac{1 + \frac{\gamma+1}{\gamma-1} \frac{P_b}{P_a}}{\frac{\gamma+1}{\gamma-1} + \frac{P_b}{P_a}} \tag{A.25}$$

Let $\gamma+1/\gamma-1 = \beta$ and therefore

$$\frac{\rho_b}{\rho_a} = \frac{1 + \beta \left(\frac{P_b}{P_a}\right)}{\beta + \left(\frac{P_b}{P_a}\right)} \tag{A.26}$$

It is to be noted that the Mach number appearing in these equations is based on the transformed velocities and can only be applied when $u_a = 0$. If $u_a \neq 0$, then one must substitute for the Mach number (V/a) the appropriate absolute velocities. From the conservation of mass through the shock

$$A = - \rho_a V_a = - \rho_b V_b \tag{A.27}$$

where the sign convention previously adopted has been used. Introducing A into equation (A.4) gives the result that

$$A = \frac{P_b - P_a}{V_b - V_a} = \frac{P_b - P_a}{u_b - u_a} \tag{A.28}$$

But A.4 may also be written as

$$A^2 \left(\frac{1}{\rho_a} - \frac{1}{\rho_b}\right) = P_b - P_a$$

to give

$$A^2 = \left(\frac{P_b - P_a}{\rho_b - \rho_a}\right) \rho_a \rho_b$$

which reduces to

$$A^2 = \frac{\left(\frac{P_b}{P_a} - 1\right)\rho_a P_a}{1 - \frac{\rho_a}{\rho_b}} \qquad (A.29)$$

Equating A.29 to the square of A.28 gives

$$(u_b - u_a)^2 = \frac{(\beta-1)\left(\frac{P_b}{P_a} - 1\right)}{\left(1 + \beta \frac{P_b}{P_a}\right)} \frac{P_a}{\rho_a}$$

which may be simplified by introducing the definition of the speed of sound to

$$u_b = u_a \pm \frac{(\beta-1)\left(\frac{P_b}{\rho_a} - 1\right) a_a}{\sqrt{(\beta+1)\left(1+\beta \frac{P_b}{\rho_a}\right)}} \qquad (A.30)$$

By the substitution in equation (A.26) of the definition of the relative velocities in terms of the absolute velocities the result

$$U = u_a \pm a_a \sqrt{\frac{1 + \beta \frac{P_b}{P_a}}{\beta + 1}} \qquad (A.31)$$

is obtained. This is, of course, equation (A.21) if $u_a = 0$.

APPENDIX B

DERIVATION OF RAREFACTION AND CHARACTERISTIC EQUATIONS

DERIVATION OF RAREFACTION AND CHARACTERISTIC EQUATIONS

In this section flows as positive to the right and negative to the left will again be considered. Referring to Fig. B-1, the rarefaction head is moving to the left.

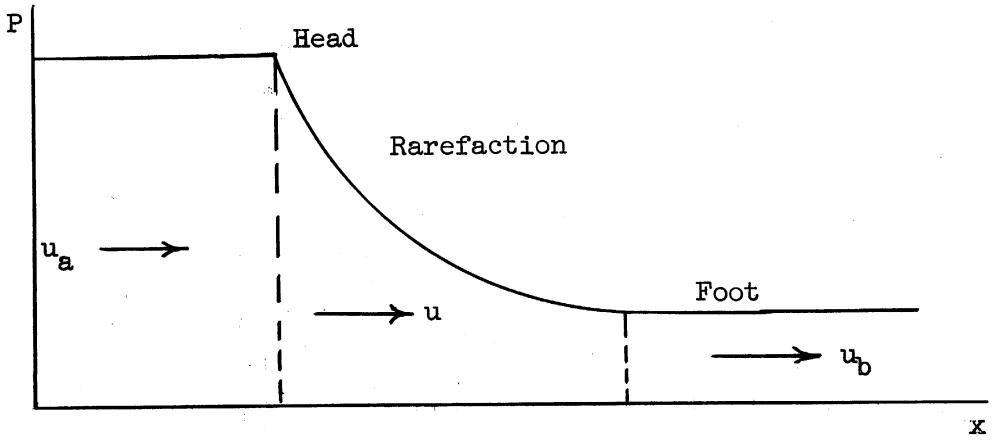

Fig. B-1. Notation for rarefaction.

At any point on the rarefaction, the velocity with respect to a stationary observed is (u-a), and let conditions at the two steady conditions in front of the head and behind the foot be designated by subscripts a and b.

Using the differential forms of the conservation laws for one dimensional, unsteady flow gives:

Mass Continuity
$$\frac{\partial \rho}{\partial t} + \frac{\partial (\rho u)}{\partial x} = 0 \qquad \text{(B.1)}$$

Momentum Continuity
$$\rho \frac{\partial u}{\partial t} + \rho u \frac{\partial u}{\partial x} + \frac{\partial P}{\partial x} = 0 \qquad \text{(B.2)}$$

Energy Balance
$$\rho \frac{\partial E}{\partial t} + \rho u \frac{\partial E}{\partial x} + P \frac{\partial u}{\partial x} = 0 \qquad \text{(B.3)}$$

Now $E = E(S,\rho)$ so that

$$\frac{\partial E}{\partial t} = T\frac{\partial S}{\partial t} + \frac{P}{\rho^2}\frac{\partial \rho}{\partial t} \quad \text{and} \quad \frac{\partial E}{\partial x} = T\frac{\partial S}{\partial x} + \frac{P}{\rho^2}\frac{\partial P}{\partial x}$$

which may be substituted into B.3 to give

$$\rho T\left(\frac{\partial S}{\partial t} + u\frac{\partial S}{\partial x}\right) + \frac{P}{\rho^2}\left(\frac{\partial \rho}{\partial x} + u\frac{\partial \rho}{\partial x}\right) + \frac{P}{\rho}\frac{\partial u}{\partial x} = 0 \qquad (B.4)$$

But the last three terms in B.4 are simply equation (B.1) and therefore

$$\frac{\partial S}{\partial t} + u\frac{\partial S}{\partial x} = 0 \qquad (B.5)$$

a result which could have been anticipated from isentropy.

From thermocynamic considerations

$$P = P(\rho,S)$$

and therefore

$$dP = \frac{dP}{a^2} - \frac{1}{a^2}\left(\frac{\partial P}{\partial S}\right)_\rho dS$$

which, upon substitution into the continuity equation B.1 yields

$$\frac{\partial P}{\partial t} + u\frac{\partial P}{\partial x} + a^2\rho\frac{\partial u}{\partial x} + 0\left(\frac{\partial P}{\partial S}\right)_\rho\left[\frac{\partial S}{\partial t} + u\frac{\partial S}{\partial x}\right] = 0 \qquad (B.6)$$

However, the bracketed terms are zero and therefore

$$\frac{\partial P}{\partial t} + u\frac{\partial P}{\partial x} + a^2\rho\frac{\partial u}{\partial x} = 0 \qquad (B.7)$$

Multiplying equation (B.2) by a and adding and subtracting from (B.7) gives the results

$$\frac{\partial P}{\partial t} + (u+a)\frac{\partial P}{\partial x} + \rho a\left[\frac{\partial u}{\partial t} + (u+a)\frac{\partial u}{\partial x}\right] = 0 \qquad (B.8)$$

$$\frac{\partial P}{\partial t} + (u-a)\frac{\partial P}{\partial x} - \rho a\left[\frac{\partial u}{\partial t} + (u-a)\frac{\partial u}{\partial x}\right] = 0 \qquad (B.9)$$

The form of the derivative operator

$$\frac{\partial}{\partial t} + (u \pm a)\frac{\partial}{\partial x}$$

is the directional derivative of the function in the directions

$$dx = (u \pm c)\, dt \qquad (B.10)$$

from which

$$dP = \pm \rho a du \qquad (B.11)$$

along the directions given by B.10.

The curves obtained by integrating B.10 are called the characteristic curves and have the simple forms

$$\begin{aligned} C_+ &: \quad x = (u+c)\, t + C_i^+ \\ C_- &: \quad x = (u-c)\, t + C_i^- \end{aligned} \qquad (B.12)$$

A wave may be said to be facing to the right if the gas travels into it from right to left and is facing left if the gas enters from left to right.

To solve for $(u_a - u_b)$, it is necessary to integrate B.11 between states a and b and apply the proper sign, or

$$u_b - u_a = \mp \int_a^b \frac{dP}{\rho a} \qquad (B.13)$$

where the positive sign applies to right facing waves and the negative sign to left facing waves. From the definition of a and the isentropic

relation connecting P and ρ, a and ρ may be eliminated. The result is

$$u_a = u_b \pm a_a (\beta-1)\left[\left(\frac{P_b}{P_a}\right)^{\frac{1}{\beta+1}} - 1\right] \qquad (B.14)$$

in which the positive sign applies to a right facing wave and the negative to a left facing wave.

To determine any of the states intermediate between a and b, equation (B.14) is applied to these states. It is often convenient for this purpose to assume values of pressure in the range between P_a and P_b and to compute the corresponding u's. The speed of sound at these points may also be readily calculated and thus the slope of the characteristic throughout the expansion zone is determined. In this way P-x-t history may be found. This is illustrated in Fig. B-2.

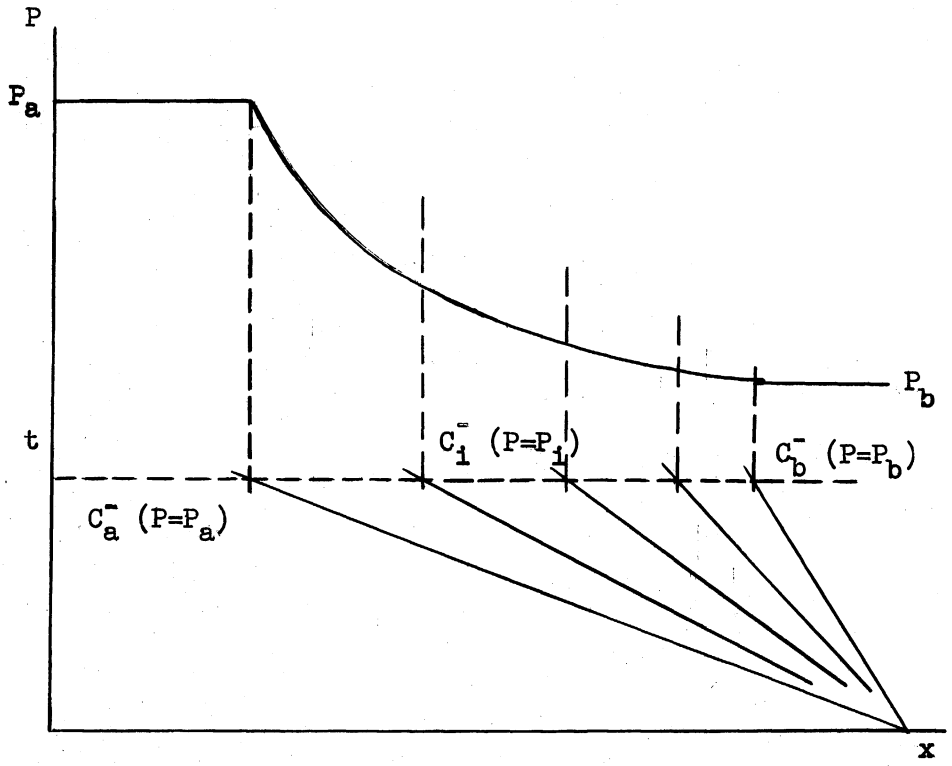

Fig. B-2. P-x and t-x plot for rarefaction wave.

APPENDIX C

DETAILED CALCULATION FOR REACTION WAVE

DETAILED CALCULATION FOR REACTION WAVE

In this section the calculation for the state behind a reaction wave will be presented. For an example, the calculation will be performed for runs 111-112. The feed gas is H_2-D_2-A with the composition given previously. The speed of sound in the unreacted mixture is computed as 1210 feet/second ($\gamma = 1.58$, $\mathcal{M} = 28$); the wave Mach number is then 6.04 and the temperature ratio is computed as

$$\frac{T_3}{T_1} = \frac{\left[2\gamma M^2 - (\gamma-1)\right]\left[(\gamma-1)\,M^2 + 2\right]}{(\gamma+1)^2\,M^2}$$

$$\frac{T_3}{T_1} = 10.98 \qquad \text{or } T_3 = 3170^\circ K$$

From the flow Mach number, the pressure ratio is computed by equation (A.21) as

$$\pi_{31} = 44.3$$

But since the initial pressure is 6 in. Hg absolute, the pressure behind the wave is 8.94 atmospheres.

Using Johnson and Long's data (25) for the dissociation of H_2, D_2, and HD, the fraction of H_2 and HD dissociated may be found

$$\text{For } H_2\text{: } \xi_{H_2} = \left(\frac{K_D}{K_D+4P}\right)^{1/2} \approx \left(\frac{.03}{8.93}\right)^{1/2} = 0.058$$

$$\text{For } D_2\text{: } \xi_{H_2} = \left(\frac{.006}{8.93}\right)^{1/2} = 0.026$$

Using the data from Circular 500 for the dissociation energies of H_2 and D_2 and assuming they are the same, Δ is calculated

$$\Delta H_f \approx 55 \text{ K cal/mole H or D}$$

From the feed composition of .143 mole fraction H_2 and .183 mole fraction D_2, the total yields of D and H are .0047 and .0083 moles respectively, based on 1 mole of mixture. If the units are maintained on a molar basis then

$$\Delta = - \frac{2(.013)(55) \times 10^3}{1.987 \times 290} = 2.5$$

However, since the amounts of H and D formed are small compared to the total quantity of material behind the wave, the gas constant for the mixture on a mass basis remains very nearly the same and the value of π_{31} for the reaction wave may be calculated from equation (75) or (76). Using values of 8.5 for the specific heats of D_2 and H_2 and 4.7 as the specific heat of argon, the values of γ and β may be found. For H_2 and D_2, $\gamma = 1.3$ and for A, $\gamma = 1.67$; for the hot mixture then $\gamma = 1.55$. This implies that $\beta_1 \approx \beta_3$ and equation (76) simplifies to

$$\pi = \frac{(3.3)(1+56.2) \pm \sqrt{[(3.3)(1+56.2)]^2+4(4.3)[(1.5)(6.04)^2(-.8)+1]}}{8.6}$$

$$= \frac{188.7 \pm \sqrt{3.56 \times 10^4 - .07 \times 10^4}}{8.6}$$

$$\pi = 43.8$$

This value is sufficiently close to the value neglecting dissociation that the properties of the wave may be considered as those of a pure shock.

The velocity behind the wave is computed as 5500 feet/second from equation (A.30). The speed of sound in the hot gas is 3960 feet/second and therefore by equation (86)

$$\overline{t'} = \frac{L}{2}\left[\frac{1}{a_3}\left(1 - \frac{u_3}{U}\right) + \frac{1}{U}\right]$$

$$= \frac{4}{2}\left[\frac{1}{3960}\ (1 - .77) + \frac{1}{7300}\right]$$

$$= 2\ [.63 \times 10^{-4} + 1.3 \times 10^{-4}] = 3.86 \times 10^{-4} \text{ secs.}$$

APPENDIX D

DERIVATION OF RATE EQUATION FOR H_2-D_2 EXCHANGE REACTION

DERIVATION OF RATE EQUATION FOR H_2-D_2 EXCHANGE REACTION

Consider the stoichiometric equation

$$H_2 + D_2 \rightleftharpoons 2HD$$

and a rate equation given by

$$\frac{d(HD)}{dt} = K_{r_1} (H_2)\ (D_2) - K_{r_2} (HD)^2 \qquad (D.1)$$

Let ξ = moles HD formed per unit volume, then

$$\frac{d\xi}{dt} = K_{r_1} \left[(A - \frac{\xi}{2})\ (B - \frac{\xi}{2}) - K^{-1}\ \xi^2\right] \qquad (D.2)$$

where K is the equilibrium constant for the exchange reaction and is equal to 4. Expanding D.2 and rearranging gives

$$\frac{d\xi}{dt} = AB - \frac{\xi}{2}(A+B) + \xi^2 (\frac{1}{4} - K^{-1}) \qquad (D.3)$$

But $\frac{1}{4} - K^{-1} = 0$ and D.3 may be integrated directly to give

$$\ln \frac{AB}{AB - \frac{A+B}{2}(HD)} = K_{r_1}\ \overline{t'} \qquad (D.4)$$

where (HD) is the product concentration of (HD) at $T = T_3$ and $P = P_3$. Solving for K_{r_1} yields

$$K_{r_1} = 2\ \frac{4.606}{\overline{t'}(A+B)}\ \log \frac{AB}{AB - \frac{A+B}{2}(HD)} \qquad (D.5)$$

BIBLIOGRAPHY

1. Becker, R., "Shock Waves and Detonation," Zeitschrift für Physik 8, 32 (1922).

2. Bennett, E. N., "Carbon Formation from Acetylene in a Shock Tube," Ae.E. Thesis, California Institute of Technology, Pasadena, 1956.

3. Bethe, H., and E. Teller, "Deviations from Thermal Equilibrium in Shock Waves," Unpublished Manuscript. Available Through University Microfilms, Ann Arbor, Michigan.

4. Britton, D., N. Davidson, and G. Schott, "Shock Waves in Chemical Kinetics: The Rate of Dissociation of Molecular Iodine," Discussions of the Faraday Society 17, 58 (1954).

5. Carrington, T., and N. Davidson, "Shock Waves in Chemical Kinetics: The Rate of Dissociation of N_2O_4," Journal of Physical Chemistry 57, 418 (1953).

6. Challis, J., "On the Velocity of Sound," Philosophical Magazine (3), 32, 494 (1848).

7. Chapman, D. L., "Rate of Explosion of Gases," Philosophical Magazine (5), 47, 90 (1899).

8. Chapman, S., and T. B. Cowling, "The Mathematical Theory of Non-Uniform Gases," 2nd Edition, University Press, Cambridge, 1952.

9. Cotter, T. P., "Collision Kinetics in Shock Waves," United States Atomic Energy Commission Report LA-1413. Technical Information Service, Oak Ridge, Tennessee.

10. Courant, R., and K. O. Friedrichs, "Supersonic Flow and Shock Waves," Interscience Publishers, Inc., New York, 1948.

11. De Groot, S. R., "Thermodynamics of Irreversible Processes," North Holland Publishing Co., Amsterdam, 1952.

12. Döring, W., "A Contribution to the Theory of Shock Waves and Detonations," Translation from the German. U. S. Air Force Technical Report F-TS-1227-IA, Air Material Command, Wright-Patterson Air Force Base, Dayton, Ohio, 1949.

13. Earnshaw, S., "On the Mathematical Theory of Sound," Transactions of the Royal Society 150, 133 (1860).

14. Elder, F. K., Jr., "Shock Wave Bibliography of Periodical Literature," APL/JHU 75-3, The Johns Hopkins University, Applied Physics Laboratory, Silver Springs, Maryland.

15. Eyring, H., et al., "Stability of Detonations," Chemical Reviews 45, 69 (1949).

16. Farkas, A., and L. Farkas, "Experiments with Heavy Hydrogen V: The Elementary Reactions of Light and Heavy Hydrogen, Thermal Conversion of D_2 and the Interaction of H_2 and D_2," Proceedings of the Royal Society A152, 124 (1935).

17. Farkas, A., "Ortho-Hydrogen, Para-Hydrogen and Heavy Hydrogen," University Press, Cambridge (1935).

18. Gilkerson, W. R., and N. Davidson, "On the Structure of a Detonation Front," Journal of Chemical Physics 23, 687 (1955).

19. Glick, H. S., W. Squire, and A. Hertzberg, "A Shock Tube Technique for the Study of High Temperature Gas Phase Reactions," Published in Reference 45.

20. Greene, E. F., "Chemical Reactions in Strong Shock Waves," Journal of the American Chemical Society 76, 2127 (1954).

21. Hirschfelder, J. O., C. F. Curtis, and R. B. Bird, "Molecular Theory of Gases and Liquids," John Wiley and Sons, Inc., New York, 1954.

22. Hugoniot, H., "On the Propagation of Motion in Bodies and Especially in a Perfect Gas," Journal de l'Ecole Polytechnique 53, 1 (1889).

23. Johnson, H., and E. A. Long, "Heat Capacity of the Simpler Gases VI," Journal of Chemical Physics 2, 389 (1934).

24. Jost, W., "Explosion and Combustion Processes in Gases," McGraw-Hill Book Co., New York, 1946.

25. Jouguet, E., "Mechanics of Explosives," O. Dour et Fils, Paris, 1907.

26. Kuethe, A. M., and J. D. Schetzer, "Foundations of Aerodynamics," John Wiley and Sons, New York, 1950.

27. Lewis, B., and G. von Elbe, "Combustion, Flames, and Explosions of Gases," Academic Press, New York, 1951.

28. Morrison, R. B., "A Shock Tube Investigation of Detonative Combustion," Ph.D. Thesis, University of Michigan, Ann Arbor, 1952.

29. Mott-Smith, H. W., "The Solution of the Boltzmann Equation for a Shock Wave," Physical Review 82, 885 (1951).

30. Prandtl, L., "Essentials of Fluid Dynamics," Hafner Publishing Co., New York, 1952.

31. Rankine, W. J. M., "On the Thermodynamic Theory of Finite Longitudinal Disturbances," Transactions of the Royal Society 160, 277 (1860).

32. Riemann, B., "Collected Mathematical Works," Teubner Verlag, Leipzig, 1892.

33. Rayleigh, Lord, "Aerial Waves of Finite Amplitude," Proceedings of the Royal Society 84, 247 (1910).

34. Rossini, F. D., et al., "Selected Values of Thermodynamic Properties," Circular 500, National Bureau of Standards, U. S. Government Printing Office, Washington, D. C., 1952.

35. Resler, E. L., Shao-Chi Lin, and A. Kantrowitz, "The Production of High Temperature Gas in Shock Tubes," Journal of Applied Physics 23, 1390 (1952).

36. Stokes, E. E., "On a Difficulty in the Theory of Sound," Philosophical Magazine (3), 33, 349 (1848).

37. Thomas, L. H., "A Note on Becker's Theory of the Shock Front," Journal of Chemical Physics 12, 449 (1944).

38. Turner, E. B., "The Production of Very High Temperatures in the Shock Tube with Application to Spectral Line Broadening," Ph.D. Thesis, University of Michigan, 1956.

39. Van Meerssche, M., "A Contribution to the Kinetic Study of the Reactions Between Atomic and Molecular Hydrogen," Bulletin Société Chemie de Belgique 60, 99 (1951).

40. Vielle, P., "On the Discontinuities Produced by the Sudden Release of a Compressed Gas," Comptes Rendus 129, 1228 (1899).

41. Zeldovich, Ya. B., "Theory of Combustion and Detonation in Gases," Academy of Sciences of the U.S.S.R., Moscow, 1944. Translated as U. S. Air Force Technical Report F-TS-1226-IA.

42. Zeldovich, Ya. B., and O. I. Leipunskii, "Obtaining Extremely High Temperatures," Journal of Physics (U.S.S.R.) 7, 245 (1953).

43. _____, "Third Symposium (International) on Combustion, Flames, and Explosion Phenomena," Williams and Wilkins Co., Baltimore, 1949.

44. _____, "Fourth Symposium (International) on Combustion," Williams and Wilkins Co., Baltimore, 1953.

45. _____, "Fifth Symposium (International) on Combustion," Reinhold Publishing Company, New York, 1955.

46. _____, "Tables and Charts for Compressible Flow," NACA Rept. 1135, U. S. Government Printing Office, Washington, (1953).

47. Zemansky, M., "Heat and Thermodynamics," 3rd Edition, McGraw-Hill Book Co., New York, 1951.

NOMENCLATURE

A = constant; arbitrary quantity; concentration of A

a = speed of sound

B = constant; arbitrary quantity; concentration of B

C = constant; arbitrary quantity; concentration of C

C_v = heat capacity at constant volume

C_{v_s} = contribution of specie s to C_v

C_p = heat capacity at constant pressure

C_{p_s} = contribution of specie s to C_p

$d\underline{V}_s$ = volume element in velocity space

$\frac{dx}{dt}$ = wave velocity

E = molecular energy of system

E_s = contribution of s to E

E_s^i = portion of E_s due to internal degrees of freedom

$f_s(\underline{r},\underline{V}_s,t);f_s(\underline{n}\cdot\underline{w}_s)$ = scalar distribution functions

H = enthalpy = $E + p/\rho$

H_o = stagnation enthalpy

H_s = contribution of s to H

H_s^o = enthalpy of formation of S at 0^oKelvin

I = an integral

$\underline{J}$ = mass flux vector

$\underline{J}_s$ = contribution of S to $\underline{J}$

K = equilibrium constant

K_r = reaction rate constant (overall)

K_s = volumetric rate of production of molecules of s^{th} type

L = length of shock tube

M = Mach number

$\mathcal{M}$ = molecular weight

m_s = mass of molecule of s^{th} type

N = total number of particles in system

n = number of samples

n_s = number density (concentration) of s

$\underline{n}$ = unit normal vector

P = hydrostatic pressure

$\tilde{P}$ = pressure tensor

$\underline{P}_{sx}$, $\underline{P}_{sy}$, $\underline{P}_{sz}$ = x, y, z components of pressure tensor due to molecules of s^{th} type

Q = defined as $Q = \rho^{-1} \sum_s m_s n_s \left(H^\circ_{s1} - H^\circ_{s2}\right)$

$\underline{q}$ = heat flux vector

$\underline{q}_s$ = contribution of s to $\underline{q}$

$\underline{q}^i_s$ = portion of $\underline{q}_s$ due to internal degrees of freedom

R_o = Universal gas constant

R = defined as $R_o/\mathcal{M}$

$\underline{r}$ = coordinate vector

S = entropy

T = temperature, absolute scale

t = time

t' = defined as $t - \frac{x_o}{U}$

U = velocity of shock wave

u = particle velocity

V = velocity in one dimensional system

V_o = mass average (stream velocity)

$\underline{V}_s$ = linear velocity of molecule of s^{th} type

$\overline{\underline{V}_s}$ = average of $\underline{V}_s$

$\underline{W}_s$ = defined as $\underline{V}_s - \underline{V}_o$

$\overline{\underline{W}_s}$ = diffusion velocity

x = coordinate in one dimensional system

x_o = initial point (for particle path)

α_g^s = number of atoms of g^{th} type in an s molecule

β = defined as $\frac{\gamma+1}{\gamma-1}$

$\Gamma_{s\sigma}^{+}, \Gamma_{s\sigma}^{-}$ = rate of production and depletion of s due to collisions involving σ

$\Gamma_{s\sigma}^{\pm} = \Gamma_{s\sigma}^{+} - \Gamma_{s\sigma}^{-}$

γ = ratio of heat capacities, C_p/C_v

Δ = $2Q/R_aT_a$

Λ = length of reservoir section

λ = coefficient of thermal conductivity

μ = coefficient of viscosity

ξ = extent of chemical reaction, defined by stoichiometry

π_{ij} = defined as P_i/P_j

ρ = mass density, mass per unit volume

ρ_s = contribution of s to ρ

Σ = summation symbol

τ = specific volume

$\underline{\psi}_s$ = flux vector associated with ψ_s

ψ_s = quantity concerned in molecular encounter

Subscripts:

0 = stagnation condition

1, 2, 3, ... = states 1, 2, 3, etc.

a, b, c, ... = states a, b, c, etc.

s = refers to molecule of s^{th} type

σ = refers to molecule of σ^{th} type

Special Notation:

Underscoring indicates vector, i.e., $\underline{A}$ = vector A

Vinculum indicates space average, i.e., $\overline{A}$ = average of A

Parenthesis indicates chemical concentrations, i.e., (A) = concentration of A